An analysis of optimal power flow strategies for a power network incorporating stochastic renewable energy resources.

Feras Alasali[a*], Khaled Nusair[b], Amr M. Obeidat[a], Husam Foudeh[c], William Holderbaum[d]

[a] Department of Electrical Engineering, The Hashemite University, Zarqa 13133, Jordan;

[b] Protection and Metering Department, National Electric Power Company, Amman 11181, Jordan;

[c] School of Aerospace, Transport and Manufacturing, Cranfield University, Wharley End MK43 0AL, United Kingdom;

[d] Aston Institute of Materials Research, Aston University, Birmingham B47ET, UK.

Abstract:

An optimal power management solution is a potential tool to develop cost effective and environmentally friendly power supply prepared using Renewable Energy Sources (RES) for the electrical power network. Therefore, the article introduces a novel optimization algorithm inspired by the vitality, namely: Manta Ray Foraging Optimization (MRFO), to figure out both multi and single objective problems of Optimal Power Flow (OPF) incorporating stochastic RES. The OPF problems are designed by considering four different objective functions: transmission power loss, emission index, fuel operational costs and voltage deviation. The stochastic and volatile nature of RES increases the complexity of the OPF issue. In this study, a new MRFO algorithm and some modern metaheuristic algorithms were used to settle the issue of OPF, enhance the energy efficiency, environment and cost performance of the power network. The test cases, with and without RES, different RES locations on the network, increasing in the load and outages of some transmission lines are considered by addressing the challenge of the proposed OPF. These cases are tested with bus systems as 30 and 118 and outcome from the suggested MRFO is compared to six metaheuristic optimization algorithms. Moreover, OPF challenges are successfully settled by the MRFO algorithm and outperform the proposed metaheuristic optimization methods.

Keywords: Optimal power flow (OPF); manta ray foraging optimization; heuristic algorithms; emission minimization, power loss; fuel cost; renewable energy.

1. Introduction

1.1. Background

In power structure, fossil fuel power generations are the main source of pollution by producing the harmful gas emissions with poor efficiency which are less than 40% [1,2]. Nowadays, the contribution of RES in the electrical power network is one of the main solutions to minimize the emission index and improve quality of power system. Considering RES, level of emissions and power quality issues in the power generation dispatch problems are turning to the crucial matter with keeping running of the modern power electrical systems [1-3]. Optimal Power Flow (OPF) including RES and fossil fuel power generations plays an important role to present a fundamental optimization problem, especially the major of the worldwide shifting towards smart and micro grids. The power network operators need to determine the optimal power generations by using OPF problem. The goal of operating power generations flow is to meet an objective function for instance minimizing gas emission, fuel operational cost and voltage deviation [4-6]. The OPF management tools are usually designed and developed to improve the efficiency, quality and stability of the power network by optimally maintaining the voltage stability and controlling the power network in cost and energy effective way. In the literature, the OPF studies [7–14] have mainly used deterministic renewable generation profiles without considering the volatile behavior of RES to solve

Preprint submitted to **International Transactions on Electrical Energy Systems.**
Corresponding author at The Hashemite University, Jordan. Email: ferasasali@hu.edu.jo (Feras Alasali).

single objective function OPF problem. Therefore, this paper aims to develop a realistic OPF model with single and multi objective functions and treat the volatile behavior of RES by developing stochastic RES system based on two probability functions , namely: lognormal and Weibull functions [2,3]. In addition, this work will examine the effect of RES locations on the power network performances.

1.2 Literature review

In literature, several optimization approaches are utilized to determine the optimal power dispatch of generation units with or without RES by solving an OPF problem. Generally, there are two types of optimization methods, traditional and intelligent optimization methods. The traditional optimization approaches, in particular quadratic programming and gradient's technique, have been mainly employed to resolve single objective OPF difficulties [10-13]. For instance, a quadratic programming method was developed and used to minimize the transmission power loss in [15] and interior point algorithm was employed to achieve optimal power generations in [7]. However, these traditional methods [7-14] are limited to the sensitivity to initial estimates, dimensions of the problem and some theoretical assumptions that are related to derivative requirements and search stagnation which helps to trap the solution at local minimum [11-14]. In modern power systems, due to the non-smooth and volatile nature of power generation problem, OPF are usually described as non-convex and nonlinear objective functions. Furthermore, the traditional optimization methods showed a lower performance in handling and solving modern power generation problems, especially with multi-objective function, due to the limitation of handling the complexity of computation and solving discontinuities and nonlinear functions [1-6]. Hence, for that case, a major development can do for a new optimization to achieve the global or near-global optimal solution to OPF challenges, which provide better capabilities compared to the traditional approaches.

Recently, various metaheuristic optimization algorithms are developed to solve stochastic optimization power flow problems with and without RES [2,3,16-23]. For example, the researchers in [3,18] developed a Particle Swarm Optimization (PSO) algorithm to resolve conflict in case of multiple objective function problem. The cost function described the fuel operational cost and emission index aimed at a power system resourced by RES [3,18]. While a Moth Swarm Optimization (MSO) method is employed in [19,20] toward resolving different objective OPF functions for IEEE 30-bus system connected to wind power generation unit. However, the proposed optimization algorithms in [19–23] have only targeted solving single objective function problems and needed an understanding about power generation with faultless in the RES. To overcome these limitations, the researchers in [24-27] proposed hybrid optimization algorithms employing self-learning techniques with heuristic algorithms. For example, the authors in [24,26] developed hybrid optimization algorithm by employing the fuzzy logic method and PSO to diminish the fuel operational cost and transmission power loss. In [27] to address the OPF problem, a self-learning technique was used to develop hybrid optimization model based on fuzzy clustering model and wavelet mutation strategy. However, the research studies in [24-27] assumed the perfect power generation knowledge for the RES without considering the volatile and non-smoothed generation nature of RES units or investigating the benefits of estimating the RES generations profiles which have a substantial influence on the performance of an electrical grid. Furthermore, due to the model complexity with different optimization techniques and the highly computational cost of these models, the hybrid optimization algorithms [24–27] suffer when the OPF includes problem multi-objective functions (very complex) or high-dimensional problem. This work aims to develop and employ number of the recent and powerful metaheuristic optimization algorithms due to the limited studies consider the significant of using metaheuristic algorithms. In general, the works on solving

power flow problems for a power network equipped with RES using metaheuristic optimization algorithms are sparse in the literature. Therefore, this paper develops a Manta Ray Foraging Optimization (MRFO) algorithm aimed at resolving both multi and single objective function problems for an electrical power network equipped with RES [28]. The MRFO model aims to treat the stochasticity of RES and create more realistic model compared to the literature [24-27] by estimating the RES based on probabilistic estimation techniques (Weibull and lognormal). Challenges in estimating the volatile RES nature substantially increase the difficulties of optimally solving OPF problem and increase the power network efficiency. The current literature has started to examine the significance of treating the uncertainty and volatility in RES to increase the energy efficiency, gas emission and fuel operational cost savings in the power networks [1-3,29,30]. The authors in [1-3,29,30] have used probabilistic estimation techniques in order to estimate the wind and solar systems considering the uncertainty and volatile nature in OPF problem by formulating a single objective function. The MRFO technique in this article aims to decrease the impact of the RES uncertainty term on the electrical network performance by minimizing the estimation error for a given OPF cost function. This paper presents a comprehensive analysis to the literature utilizing six recent metaheuristic algorithms as part of modern optimization algorithms compared to the proposed MRFO algorithm [28]. This analysis investigates the optimization methods performance for single and multi objective function taking into account the stochastic RESs. The MRFO algorithm will be compared to powerful and modern metaheuristic optimization algorithms stochastic from the literature: Chaotic Gravitational Search Algorithm (CGSA) [31], Supply Demand-based Optimization (SDO) [32], Improved Particle Swarm Optimization (IPSO) [33], Ant Lion Optimization (ALO) [34], Moth-Flame Optimization (MFO) [35], Autonomous Groups Particles Swarm Optimization (AGPSO) [33]. These new optimization algorithms aim to provide highly efficient algorithms for solving complex engineering problems and achieving global solution. The proposed new metaheuristics algorithms outperformed the common algorithm such as PSO over well-studied and engineering problems. Therefore, the CGSA, SDO, IPSO, ALO, MFO and AGPSO algorithms can be powerful and efficient in solving single and multi-objective functions for OPF cases for a power network system equipped with RES. The researches on solving power flow problems for a network connected to RES using metaheuristic optimization algorithms are sparse in the literature and there is limited studies introduce the impact of RES on the power network or the performance of the optimization algorithms or employ and compare different new metaheuristic optimization algorithms [36]. For example, the Success History-based Adaptive Differential Evolution (SHADE) algorithm has been used by Biswas *et al.* [37] to solve OPF for a power network (IEEE-30 bus system) connected to only wind power sources. In [37], Biswas *et al.* the SHADE algorithm used to solve two main OPF problems, generation costs and power loss, without taking into account the other OPF problems such as the voltage deviation. Furthermore, the proposed power network in [37] is only included the wind power sources in fixed location without considering the impact of other RES such as solar systems as one of popular RES in the world. In our paper, the stochastic behavior of both wind and solar power generation units are considered with different locations which increased the complexity of solving the OPF problems.

Generally, heuristic optimization algorithms aim to achieve the global or near global optimal solution for the objective function by searching a wide variable space that are not close to the current state, which needs extensive search and to be a random process as possible. However, for OPF problem with multi objective function and volatile RES nature, the computational cost of these models will be high with restricted ability to achieve global optimal point in efficient time and it is very complex to implement and handle real-world problems [28]. This

motivated Weiguo Zhao et al. [28] to employ a new heuristic optimization method called Manta Ray Foraging Optimization (MRFO) algorithm. This new metaheuristic technique requires few adjustable parameters compared to the other techniques (s), so it consumes less time and easy to implement, which helps this algorithm to be potential for engineering applications and solving real-world problems. In [28], the MRFO is bio-inspired algorithm and developed based on the intelligent activities of manta rays, which includes three unparalleled foraging schemes, namely: chain, cyclone, and somersault. This new optimization algorithm aims to introduce an efficient approach for solving and handling different real and actual engineering challenges and problems such as designing pressure vessel and tension/compression spring. The performance of MRFO is evaluated throughout 23 well-known test functions and 8 benchmark actual engineering problems [28]. The MRFO algorithm performance results show a powerful ability to achieve global optimization solution for constrained and unconstrained engineering problems. Furthermore, the evaluation of the MRFO algorithm shows that this proposed algorithm reduces the computational cost which helps it to be very suitable for real-world engineering problems [28]. Therefore, the MRFO algorithm can be beneficial for complex OPF with multi objective function and handling the volatile nature of RES in modern power system network. Adequate stochastic optimization models for modern network equipped with RES have gained a significant interest worldwide due to the prospect benefits of improving the environmental, energy and cost saving performance. In this work, a stochastic estimation model for RES and new MRFO algorithm will help to improve the power quality and environmental performance by reducing gas emissions, voltage deviation, fuel cost, and transmission loss. To the best of our knowledge, there are no studies on solving power flow problems and energy optimization problems have used the MRFO for solving OPF problems considering the volatile nature of RES or investigating the effect of increasing the demand system, power outages and RES locations in the power network.

1.3 Contributions

In this work, a new MRFO algorithm has been developed and presented incorporating with a stochastic probability prediction model for RES. The proposed MRFO algorithm is compared to six metaheuristic optimization methods for solving OPF problem in grid connected to RES. The proposed metaheuristic and MRFO methods have been designed to minimize voltage deviation, gas emission, fuel cost and the power loss on two scales of power networks, IEEE 30-bus and 118-bus. In this work, the MRFO algorithm has been compared to new powerful optimization algorithms (CGSA, SDO, IPSO, ALO, MFO and AGPSO) as highly efficient algorithms for solving complex actual engineering problems. To the author's knowledge, the MRFO has not used on solving power flow optimization problems and compared to the new proposed metaheuristic optimization algorithms (CGSA, SDO, IPSO, ALO, MFO and AGPSO), unlike the literature [19-26] that only employed one optimization method or only comparted to common algorithm's. This article targets to fill the gap in the previous literature by investigating the impact of RES locations, increasing the level of demands and power system outages on the power network performance. The originality of this article is laid out in the following points:

i. A new MRFO optimization model is developed and employed to solve and handle complex OPF problems (single and multi-objective function) considering the uncertainty and stochastic behavior of RES by using probabilistic estimation model.
ii. Unlike the literature, new metaheuristic optimization models (CGSA, SDO, IPSO, ALO, MFO and AGPSO) are developed and employed to solve OPF problems and compared to MRFO considering the stochastic nature of renewable energy resources.

iii. Unlike the previous studies [24-27] that focused only on solving OPF problem with single objective function, this paper aims to provide a comparison analysis for new heuristics optimization algorithms on solving single and multi-objective functions for electrical networks equipped with or without stochastic RES.

iv. A comparison analysis for the impact of increasing the electrical demand, power system outages, locating RES based on different scenarios is presented to examine and evaluate the performance of the proposed algorithms using different real power network operation conditions.

1.4 Outline of paper

The rest of this study is structured as follows: the OPF problems and the probability prediction models for RESs formulations are detailed and introduced in Section 2. The MRFO algorithm is presented in Section 3. The simulation results, comparisons and discussions are presented in Section 4. Finally, the summary of this paper and conclusions are highlighted in Section 5.

2. Problem Description: Components and mathematical formulation

The OPF problems for an electrical power network incorporating with RES are nonlinear, complex and non-convex optimization problems, where the aim is to find the optimal generations mix of conventional generations and RES. Table 1 presents the objective function for our OPF problems that has been divided into 7 cases including single and multi-objective functions. These functions are solved under number of equality and inequality limitations and constraints, as will be discussed in subsections 2.1. Finally, the probabilistic estimation model for RES is presented in subsection 2.2 to generate solar and wind power profiles.

Table 1: The description and summary of the objective functions for OPF problems.

Case number	Objective function
1	minimization of transmission power loss.
2	minimization of emission index.
3	minimization of fuel operational cost.
4	minimization of voltage level deviation.
5	minimization of fuel opertional cost and voltage level deviation.
6	minimization of fuel operational cost and transmission power loss.
7	minimization of emission index, fuel opertional cost, voltage deviation, transmission power loss.

2.1 Optimal Power Flow (OPF) Problems and model constraints

In this article, the OPF problems for the electrical networks models under study incorporating with RES have 7 objective functions [2,3], as presented in Table 1. The multi objective function (Cases 5,6 and 7) are introduced in this section as the total production cost for single functions. The objective functions listed in Table 1 are expressed as:

1- Power transmission loss:

The total transmission line loss in the proposed power network systems, P_{tl}, is commonly described through Equation (1) from all types of resources [3].

$$P_{tl} = \sum_{q=1}^{W} G_q\left({V_i}^2 + {V_j}^2 - 2V_iV_j\ \cos\left(\theta_i - \theta_j\right)\right) \quad (1)$$

where P_{tl} is the summation of power loss over all network load buses and transmission lines, W is the total number of the power transmission lines and load buses, V_i and V_j are the terminal voltages magnitudes of branch q, θ_i and θ_j are the terminal voltage angles of branch q and G_q is the conductance of branch q.

2- Emission index:

The conventional generation units run using release fossil fuel sources are the main source of pollution by producing the harmful gas emissions into the atmosphere. In order to limit emissions and avoid carbon tax penalties, the power network operators work on improving the environmental performance of the networks by minimizing the producing gas emission. This objective aims to reduce the total gas emission, E_g, in the proposed networks without affecting the total power generations under different operation and load conditions. The E_g is expressed in tons per hour by Equation (2) [2].

$$E_g = \sum_{n=1}^{NG} \left(\alpha_n + \beta_n P_n + \gamma_n {P_n}^2\right) \tag{2}$$

here, the E_g is the total gas emissions, NG is the number of thermal generation units, α_n , β_n and γ_n are the emission index coefficients for the *n* thermal power generation unit and P_n the power generated from thermal unit *n*.

3- The fuel operational cost:

The fuel operational cost of all thermal units, C_{fuel} , is described in Equation (3) using a quadratic function as presented in [1-4].

$$C_{fuel} = \sum_{n=1}^{NG} \left(\lambda_n + \delta_n P_n + \varphi_n {P_n}^2\right) \tag{3}$$

in this equation, C_{fuel} is the fuel operational cost for the NG of thermal power generation units, λ_n , δ_n and φ_n are the coefficients of the fuel operational cost for the n thermal generation unit and P_n the power generated from thermal unit n.

4- Voltage level deviation:

In order to examine and evaluate the proposed optimization algorithms in this paper under power quality terms, the voltage deviation index is used. The voltage security in electrical networks is one of the most common power quality terms and operators aim to minimize generating an unattractive voltage profile. The voltage deviation index, V_D , is basically the summation of all voltage deviation between the load bus, V_l, for all buses, *L*, and the rated voltage which equal to 1.0 per unit. The cost function for the voltage level deviation is defined in Equation (4) as presented in [2,3]:

$$V_D = \sum_{l=1}^{L} |V_l - 1| \tag{4}$$

5- Fuel operational cost and voltage level deviation.

The multi cost function is basically the total of single functions. In Equation (5), the fuel operational cost and voltage level deviation index is described [2,3].

$$C_{FV} = \left(\vartheta_f \sum_{n=1}^{NG} \left(\lambda_n + \delta_n P_n + \varphi_n {P_n}^2 \right) \right) + \left(\vartheta_{VD} \sum_{l=1}^{L} |V_l - 1| \right) \quad (5)$$

here, C_{FV} is the multi objective function (fuel operational cost and voltage level deviation) in a power network, $\vartheta_f$and ϑ_{VD} are weight factors for each function and they assumed to be equal to 1 and 100 [1-4], respectively. In Equation (5), the weight factors (ϑ_f and ϑ_{VD}) are optimality selected and they are common values for the proposed network [2,3]. In general, for the multi objective functions in this work, the weighted sum strategy is used in this paper as one of the most common and popular multi objective functions techniques. The weighted sum strategy aims to convert the objective (optimization) problems into scalar problems through scaling operation process and then adding weighted factors for all the objectives. In order to obtain the real values of the objective function, it will need to reverse the scaling process.

6- *Fuel operational cost and power transmission loss.*

The fuel operational cost and the power transmission loss functions are merged in a cost function, C_{FP}, as presented in Equation (6) [2,3].

$$C_{FP} = \left(\vartheta_f \sum_{n=1}^{NG} \left(\lambda_n + \delta_n P_n + \varphi_n {P_n}^2 \right) \right) + \left(\vartheta_P \sum_{q=1}^{W} G_q \left({V_i}^2 + {V_j}^2 - 2V_i V_j \cos\left(\theta_i - \theta_j\right) \right) \right) \quad (6)$$

where ϑ_f and ϑ_P are weight factors for fuel operational cost and power transmission loss functions and they assumed to be 1 and 40 [16], respectively. In Equation (6), the multi objective function form for fuel cost and loss is one the common and standard from for the proposed network. The weighted sum strategy is used in this equation to present the multi objective function problem as common and popular multi objective functions strategy. In addition, the weight factors (ϑ_f and ϑ_P) are optimality selected and they are common values for the proposed network [2,3].

7- The fuel operational cost, power transmission loss, gas emission index and voltage level deviation.

In order to examine the proposed optimization methods with a conflict and complex objective function, this case merges four contrasting cost functions. In Equation (7), the fuel operational cost, gas emission, power transmission loss and voltage level deviation functions are emerged as multi cost function as follows:

$$\begin{aligned} C_{FPGV} = & \left(\vartheta_f \sum_{n=1}^{NG} \left(\lambda_n + \delta_n P_n + \varphi_n {P_n}^2 \right) \right) + \left(\vartheta_P \sum_{q=1}^{W} G_q \left({V_i}^2 + {V_j}^2 - 2V_i V_j \cos\left(\theta_i - \theta_j\right) \right) \right) \\ & + \left(\vartheta_g \sum_{n=1}^{NG} \left(\alpha_n + \beta_n P_n + \gamma_n {P_n}^2 \right) \right) + \left(\vartheta_{VD} \sum_{l=1}^{L} |V_l - 1| \right) \end{aligned} \quad (7)$$

in this equation, ϑ_g is a weight factor for the gas emission index and it equals 19 [2,3], whileϑ_f, ϑ_P , ϑ_{VD} are assumed here to be 1, 22 and 21 [2,3], respectively. Similar to Equations (5) and (6), the weighted sum strategy is used in Equation (7) to present the multi objective function problem for the fuel operational cost, power transmission loss, gas emission index and voltage level deviation.

2.1.1 The power network constraints

The OPF as optimization problems for electrical network systems has a number of physical constraints and limits. The power network limitations are normally related to the operation conditions for the network equipment's and model parameters for instance frequency, current and voltage. These limitations are basically obtainable and divided into equality and inequality constraints.

(a) Equality Constraints:

In OPF problems, the equality limitations and constraints typically define the load flow in a power network system. In Equations (8) and (9), the total generates active power, $\sum_{n=1}^{NG} P_n$, and reactive power, $\sum_{n=1}^{NG} Q_n$, produced from all available thermal and RES generations units, NG [1-4].

$$\sum_{n=1}^{NG} P_n = P_D + P_{tl} \tag{8}$$

$$\sum_{n=1}^{NG} Q_n = Q_D + Q_{tl} \tag{9}$$

where P_D and Q_D represent the power demand of total active and reactive, P_n and Q_n represent the power of active and reactive generated from a generation unit n, P_{tl} and Q_{tl} represent the power loss of total active and reactive over all grid load buses and lines, respectively. In addition, the load flow constraints for the proposed electrical network system can be described as follow [2]:

$$P_n - P_{D\,n} = V_n \sum_{q=1}^{W} V_q \left(G_{nq} \cos\theta_{nq} + B_{nq} \sin\theta_{nq}\right) \tag{10}$$

$$Q_n - Q_{D\,n} = V_n \sum_{q=1}^{W} V_q \left(G_{nq} \sin\theta_{nq} + B_{nq} \cos\theta_{nq}\right) \tag{11}$$

Here, $P_{D\,n}$ and $Q_{D\,n}$ are the power demand of total active and reactive connected to generation unit n, the P_n and Q_n, V_n and V_q represent a voltage magnitudes at buses n and q, G_{nq} is the conductance between terminal buses n and q, B_{nq} represents a transfer susceptance among terminal buses n and q, $\theta_{nq}$is the voltage angle variance among terminal buses n and q.

(b) Inequality Constraints:

Generally, the power network operating limitation related to the power system equipment's are mainly inequality constraints. The inequality constrains can be expressed as the following [2,3]:

- Power generation constraints including thermal and RES.

$$V_{n\,(\min)} \le V_n \le V_{n\,(\max)}\ ,\ \text{n = 1,2,...,NG} \tag{12}$$

$$P_{n\,(\min)} \le P_n \le P_{n\,(\max)},\ \text{n = 1,2,...,NG} \tag{13}$$

$$Q_{n\,(\min)} \le Q_n \le Q_{n\,(\max)},\ \text{n = 1,2,...,NG} \tag{14}$$

where $V_{n\,(\min)}$ and $V_{n\,(\max)}$ represent both minimum and maximum voltage at generation unit n, $P_{n\,(\min)}$ and $Q_{n\,(\min)}$ for a minimum active and reactive power generation at unit n, $P_{n\,(\max)}$ and $Q_{n\,(\max)}$ for a maximum active and reactive power generation at unit n, respectively.

- The power transformer tap setting limitation.

$$PT_{k\,(\min)} \leq PT_k \leq PT_{k\,(\max)},\ \text{k = 1,2,...,NT} \tag{15}$$

where the PT is the power transformers tap setting, the minimum and maximum setting limitation are $PT_{(\min)}$ and $PT_{(\max)}$, recpectively, and k the regulating tap of the transformer and NT is the number of taps.

- The voltages level limitations at load buses, Equation (16) and the transmission loading limitations, Equation (17).

$$VL_{b\,(\min)} \leq VL_b \leq VL_{b\,(\max)}\ ,\ \text{b = 1,2,...,NL} \tag{16}$$

$$TL_r \leq TL_{r\,(\max)},\ \text{r= 1,2,...,Ln} \tag{17}$$

where VL_b is the magnitude of voltage at bus b, NL is the total number of buses, $VL_{b\,(\min)}$ and $VL_{b\,(\max)}$ are the minimum and maximum voltages at the load bus b, TL_r is the loading magnitude at transmission line r, Ln is the number of transmission lines and $TL_{r\,(\max)}$ is the maximum loading at transmission line r.

(c) Handling equality and inequality limitations and constraints

To handle inequality constraints and decline any infeasible solutions, an external penalty function is employed and applied in this article [2,3]. This penalty function aims to penalize infeasible solution and keep the constraints dependent variables within the acceptable values during the iterative searching process. Consequently, the constraint OPF problems (Equations 1 to 7) can be converted into unconstrained optimization problem using a penalized cost function to each equation. The penalized objective function is defined as [2,3]:

$$C_{penalty} = Z_P\left(P_1 - P_{1(\lim)}\right)^2 + Z_Q\sum_{n=1}^{NG}\left(Q_n - Q_{n(\lim)}\right)^2 + Z_V\sum_{l=1}^{L}\left(V_l - V_{l(\lim)}\right)^2 + \ Z_{TL}\sum_{r=1}^{Ln}\left(TL_r - TL_{r(lim)}\right)^2 \tag{18}$$

where Z_P, Z_Q, $Z_V$and Z_{TL} are the penalty factors for inequality constraints and they are assumed to be in this paper 100, 100, 100, and 100,000, respectively as presented in [1-3], P_1 is the active power magnitude at the slack bus, $P_{1(\lim)}$ is the limit value of P_1, $Q_{n(\lim)}$ is the reactive power limit at Q_n, the limit value of voltage bus V_l is $V_{l(\lim)}$, the limit value of the transmission line loading TL_r is $TL_{r(\lim)}$.

2.2 The probabilistic estimation model for RES

In order to improve the reliability and quality of an electrical networks, RES has been widely employed. Nowadays, RES has a direct impact on the electricity market [2,29,30]. In a power system incorporating with RES to solve OPF problem, for instance reducing gas emissions index, it is vital to optimally rise the power output from RES. However, the RES is naturally volatile and basically depends on weather conditions [29,30]. Therefore, a stochastic estimation model for RES profiles instead of deterministic profiles is essential to efficiently and optimally solve OPF problems with RES. The stochastic estimation model helps the optimization algorithm to deal with the uncertainties in RES profiles. In this article, the wind and solar energy sources are the most popular RES connected in different location scenarios to two power networks (IEEE 30-bus and 118-bus). The difficulties in accurately predicting the weather condition increase the challenge of optimality solving OPF problem with RES. In this work, the RESs (wind and solar power generations) have been modelled by using probabilistic

estimation algorithms to generate the RES profiles and present the stochastic nature. In OPF problems, the wind and solar generation profiles are utilized as a negative load to allow the available RES power to be firstly injected to the network then the rest of generation units. This means that the total demand will be reduced, which minimizes the gas emission, fuel operational cost and power loss of the thermal units. In addition, the RES units dispatch the optimal power value which optimally solves the OPF problem at each case.

2.2.1 Wind Power Units

The generation of wind power units are guided by weather condition such as the wind speed. Therefore, the generation power profile of wind power units can be descried as stochastic term. The wind power units basically depends on one main variable, the wind speed, which follows the Weibull probability distribution function [2,29,30]. Thus, the wind generation output can be characterized and presented as a random variable. The probability of wind speed based on Weibull function, $W_s(v)$, is described in Equation (19) as presented in [2,3,29]. The Weibull probability estimation for the wind speed delivers the uncertainty term in the wind power output.

$$W_s(v) = \frac{\kappa}{s}\left(\frac{v}{s}\right)^{\kappa-1} e^{-\left(\frac{v}{s}\right)^{\kappa}} \tag{19}$$

Here, v is the wind speed, κ is the dimensionless shape factor and s is the scale factor of the Weibull distribution function. The wind generation unit converts the wind kinetic energy to electrical energy, as described in Equation (19). By using the estimated value of the wind speed, v , the electricity power output from the wind generator unit, $W_p(v)$, can be calculated as in [2,3,29].

$$W_p(v) = \begin{cases} 0 & v < v_{in} \; and \; v > v_{out} \\ W_{pr}\left(\dfrac{v - v_{in}}{v_r - v_{in}}\right) & v_{in} \le v \le v_r \\ W_{pr} & v_r < v \le v_{out} \end{cases} \tag{19}$$

where W_{pr} is the nominal and rated power value for the wind generation unit, v_r is the rated and nominal wind speed, v_{in} and v_{out} are the cut-in and cut-out wind speed for the proposed wind generation unit, respectively. The impact of locating the wind generation unit in different location scenarios on the power flow results will be investigated in this work. In this article, the cost of generated electricity by wind power generation units is described and formulated as presented in [2,3,29,30] by using the wind speed and actual power profiles. The total power generation from wind units, PW_{cost}, is the summation of the direct, reserve and penalty costs of the wind units, W_D , W_R, and W_P , respectively in ($/h) [2,3,24] as described in Equation (20), if N is the total number of wind units. The penalty term, W_P, aims to minimize the impact of the wind generation uncertainty on the cost estimation.

$$PW_{cost} = \sum_{n=1}^{N} W_{D,n} + W_{R,n} + W_{P,n} \tag{20}$$

2.2.2 Solar Power Units

Solar power profile mainly depends on the weather condition such as solar irradiance; therefore, it is uncertain and volatile quantity. Solar irradiance follows the lognormal probability distribution function, which means that the solar system output is a random variable. The probability of solar irradiance based on lognormal function, S (I), is described in Equation (21) as presented in [2,3]. The lognormal estimation for the solar irradiance delivers the uncertainty term in the solar power output.

$$S(I) = \frac{1}{I\sigma\sqrt{2\pi}} \exp\left(\frac{-(\ln I - \mu)^2}{2\sigma^2}\right) I > 0 \tag{21}$$

where I is the solar irradiance, μ and σ are the mean and standard deviation of the lognormal probability function. The solar power generation unit converts solar irradiance to electrical energy, where the solar system output, $S_p(I)$, is calculated using the estimation of solar irradiance and presented in Equation (22) [2,3].

$$S_p(I) = \begin{cases} S_{pr} \dfrac{I^2}{I_s R_c} & for \quad 0 < I < R_c \\ S_{pr} \dfrac{I}{I_s} & for \quad I \geq R_c \end{cases} \tag{22}$$

Where S_{pr} is the nominal power output of the solar generation unit, I_s is the standard solar irradiance equal to 800 W/m^2, R_c is the irradiance point which is set equal to 120 W/m^2 as in [2,3,29,30]. The total power generation costs of PV units,PV_{cost}, is mainly calculated similar to wind power systems using the direct, reserve and penalty costs of PV system, PV_D , PV_R, and PV_P respectively in ($/h) [2,3,24] as described in Equation (23), if k is the total number of PV units [2,3, 24]. Finally, the impact of locating the solar generation unit in different location scenarios at power network on the power flow will be investigated in this paper.

$$PV_{cost} = \sum_{i=1}^{K} PV_{D,k} + PV_{R,k} + PV_{P,k} \tag{23}$$

In general, the total cost of all generation units (fuel, wind and solar) for the proposed power network model, T_{cost}, in $/h is presented using a common function in Equation (24) that is presented in [2,3, 29,30] as

$$T_{cost} = C_{fuel} + \mathrm{PW_{cost}} + PV_{cost} \tag{24}$$

3. Proposed method: Manta Ray Foraging Optimization

In 2019, a new bio-inspired and metaheuristic optimization algorithm called Manta Ray Foraging Optimization (MRFO) has been introduced by Weiguo Zhao *et al.* [28]. The aim of MRFO is to deliver an alternative optimization approach for handling engineering problem and challenges. In addition, the MRFO algorithm is simple to develop and implement with lower running simulation time, where it required few adjustable parameters compared to other optimization algorithms [28]. The MRFO algorithm provide is highly efficient algorithm for solving complex engineering problems and achieving global solution [28]. The MRFO algorithm outperformed common algorithms in [28] over well-studied and engineering problems. Therefore, the MRFO algorithm can be powerful and efficient in solving single and multi-objective functions for OPF cases for

a power network system equipped with RES. The basic idea of MRFO is inspired and developed from the intelligent activities and natures of manta rays by creating three unique foraging strategies, chain, cyclone and somersault. These strategies present the search characteristics of manta rays and work on facilitating and smoothing convergence to the global solution [28]. Firstly, the chain foraging strategy updates the current searching position based on the current global best solution. Secondly, the random searching performance is presented by cyclone foraging strategy to improve the extensive global search mechanism. This strategy works on adding a random position (random searching) in the search space to update each individual position to the random and the reference positions. The first step participates in exploitation and the following step in exploration. The MRFO algorithm allows to smoothly change between the chain and the cyclone foraging's by write either gradually increasing the value of rand, the ratio between current and maximum number of iterations. Finally, the somersault foraging is a strategy allows each individual to move from the existing or actual position to any symmetrical position around the current global solution. The MRFO algorithm for solving optimization problems is summarized in Figure 1 and described below:

- **Step 1 Population Initialization**: this step aims to generate a random population in the domain of the optimization problem. This step is basically similar to another heuristic optimization algorithm.
- **Step 2 Searching Step**: at each iteration, t, the position of each individual in the domain will be updated based on the current searching position and reference position. The value of the ratio between the current iteration, t, and maximum iterations number (T) decreases from (1/T) to 1 which means moving from exploratory to exploitative search, respectively.
- **Step 3 Reference Position Evaluation**: the current global best solution is selected to be a reference position for the utilization of search when the ratio of t/T is less than the random value. When the ratio of t/T is larger than the random value, a random value from space will be selected as reference position.
- **Step 4 Moving between Strategies in MRFO**: the MRFO can change between the chain and the cyclone foraging based on the random value. Then, individuals in the domain will be updated based on their current positions and the current global best solution by using somersault foraging.
- **Step 5:** Repeat steps 2–4 until the maximum iterations number is reached, which is the stop criterion here.

In general, MRFO algorithm is required to adjust few numbers of parameters which helps it to be an easy algorithm to implement and makes it very potential for engineering applications. The parameters of MRFO algorithm are related to the foraging strategies, where there are two main weight coefficients to adjust the chain and cyclone foraging strategies Additionally, two random numbers will be used to update the individual position in somersault foraging. The computational cost of heuristic optimization models is basically dependent on the number of parameters (variables, individuals) and the maximum iterations number [28]. In this paper, the best solution (optimal values) for each parameter was selected over range of values to achieve the results in this work. The simulation models for the MRFO and other heuristics optimization algorithms have been implemented based on the parameters and the details are presented within the following section.

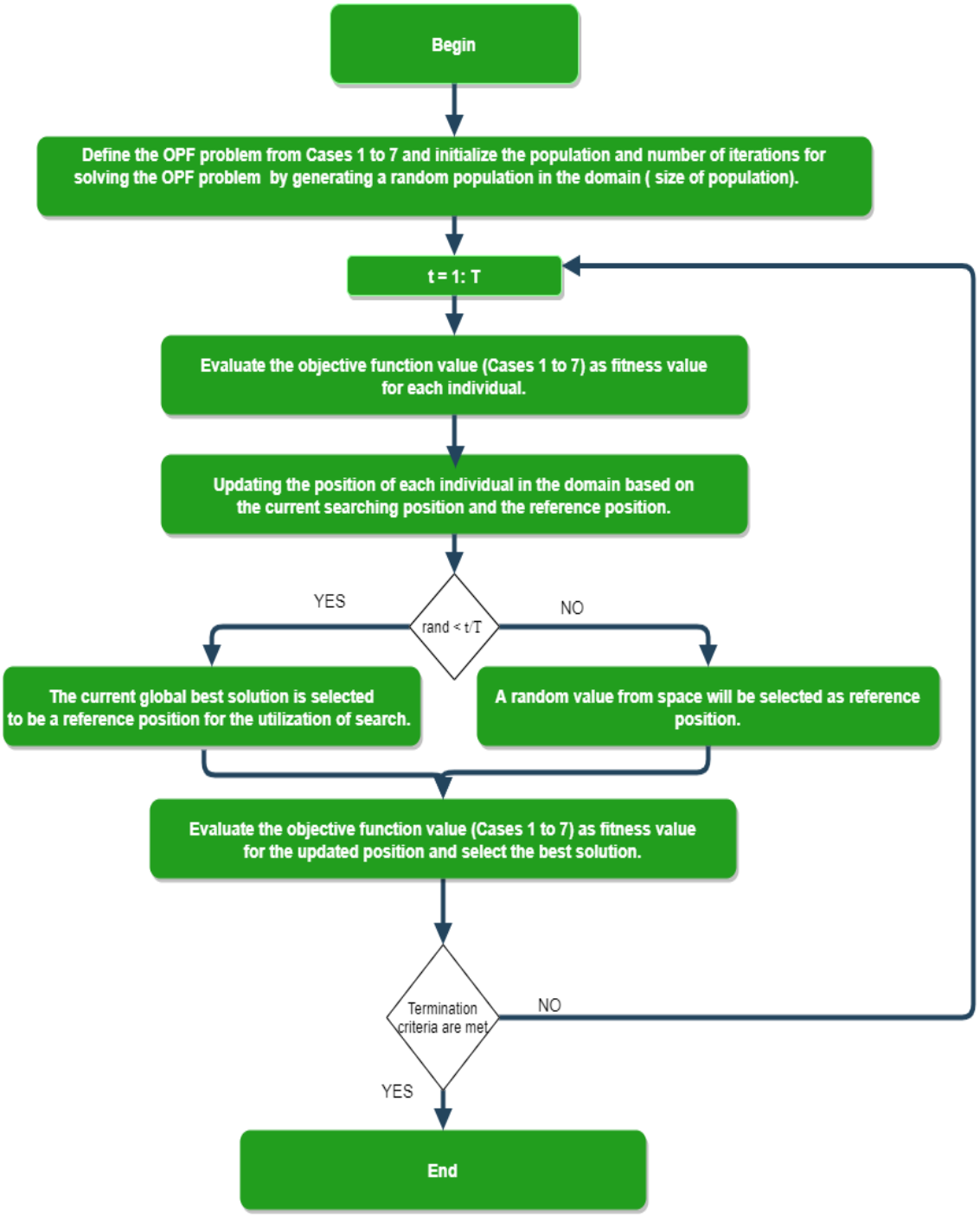

Fig. 1. The main MRFO procedures.

4. Simulation results and discussion

The suggested formulation for OPF problems in electrical networks equipped with RES, as discussed in Section 2, is tested to examine the performance of MRFO approach. Thus, this section presents and discusses the results of the suggested optimization approaches. Firstly, the description of the test systems is introduced; then, the MRFO and other heuristics optimization algorithms tested under different power network and operation scenarios. Throughout this section, the proposed MRFO optimization approach is comparable against six heuristics optimization algorithms from the literature, specifically: CGSA [31], SDO [32], IPSO [33], ALO [34], MFO [35],

and AGPSO [33]. The comparison of single and multi-objective function for OPF problem over different network scenarios are presented.

4.1 Test systems

For the purpose of examining the potency and evaluating the performance of the suggested optimization algorithms, all algorithms are using two standard power network systems, IEEE bus systems as 30 and 118. Firstly, the IEEE 30 is adopted as a reference model for electrical power grid here in the article from [38-40]. The IEEE 30-bus system includes a six thermal power generation parts, 30 buses, 41 branches and the swing bus is bus 1, as presented in Figure 2. The thermal generations locate to be at buses number 1, 2, 5, 8, 11 and 13. The magnitude limitation of load voltage represents a 0.95–1.05 p.u and with generator voltage limits are 0.95–1.1 p.u. In the buses number 11,12,15 and 36, transformers with tap changer that vary the voltage from 0.9 p.u. toward 1.1 p.u. Furthermore, the voltage automatic regulator compensators limits are 0 - 0.5 p.u. In this network, the active demand equal to 2.834 p.u and for a reactive equal to 1.262 p.u, besides a total load is 100 MVA. To investigate and examine the impact of incorporating RES to the proposed network system and RES locations on the OPF solvers, the IEEE 30-bus system [38-40] is adjusted with inserting RES in two different locations, as follows:

- The IEEE 30-bus system is adjusted by firstly adding and incorporating solar and wind generation unit at bus 24 and 30, respectively. Secondly, the thermal generation units have been replaced through solar unit next to buses number 5, also number 13, and wind system by bus number 11, as presented in Figure A.1 in the appendix section. The details and data model for wind and solar systems are adopted form [2,3] and presented in Table 2 and it's called IEEE 30-bus Modified (1).
- In order to examine the proposed optimization solvers performance across diverse scenarios of RES locations, the IEEE bus number 30 Modified (2) is used in this section, as presented in Figure A.2. The thermal generation units in IEEE 30-bus system replaced with solar unit next to buses number 5 with number 13, and wind system by bus number 11. In this modification, solar and wind systems have been added to buses 17 and 28, respectively. The general RES model conditions and data of wind and solar systems are described in Table 2 [2,3]. Secondly, for assessing the MRFO algorithm in terms of both scalability and reliability, an IEEE bus for 118 in power network is employed with large-area power network model. The data and network specification for IEEE 118-bus system are extracted from [39].

Both of the IEEE power network systems are used to present and formulate OPF problems, as presented in Section 2. The coefficients of fuel cost and gas emission function equations, as presented in Section 2.1, are described in Table 3 and given in [2,3,32,34]. To implement the proposed MRFO and the other six heuristics optimization algorithms, a certain number of parameters needs to be firstly selected to achieve the best optimal solution. Generally, the performance of optimization techniques relies on factors such as the model parameters, the complexity of the problem, constraints, the information availability, and the simulation model package. Moreover, each optimization algorithm has advantages and disadvantages and there is no algorithm suitable for all problems. In this article, the values of the parameters are verified based on empirical tests using previous studies information and running the proposed optimization solvers many times over a range of values for each parameter. The main parameters of each optimization technique are presented in Table 4 and including the range and optimal values. The best solution (optimal values) for each parameter was chosen to achieve the results in this work. The simulation models for the MRFO and other heuristics optimization algorithms have been employed and developed on MATLAB 2016 using 2.8-GHz i7 PC with 16 GB of RAM.

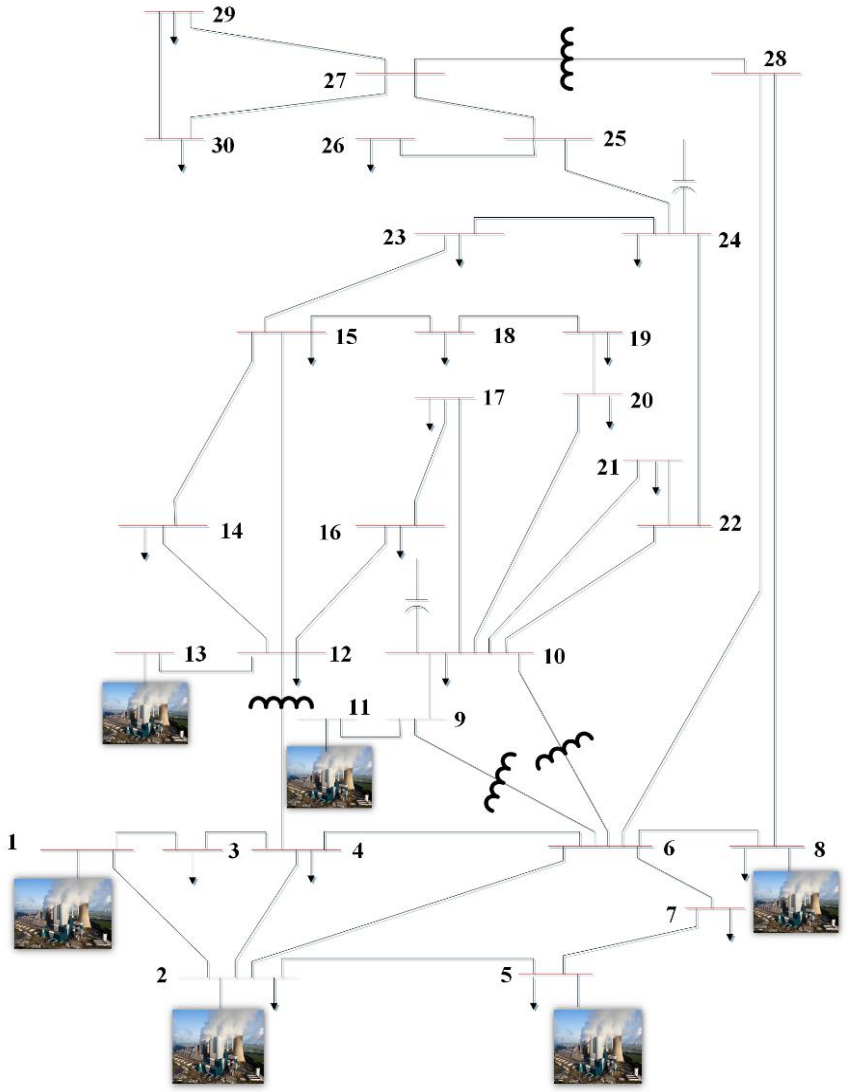

Fig. 2. The proposed IEEE 30-bus network

Table 2: The data of solar and wind systems for the proposed Modified (1) and (2) networks.

Wind systems connected to the proposed Modified (1) network.								
Unit	Bus	No. of turbines	W_{pr}	s	κ	v_{in} (m/s)	v_{out} (m/s)	v_r (m/s)
1	11	10	2	9	1.65	4	25	13
2	30	12	2	10	1.7	4	25	13
Wind systems connected to the proposed Modified (2) network.								
1	11	10	2	9	1.65	4	25	13
2	28	12	2	10	1.7	4	25	13
Solar systems connected to the proposed Modified (1) network.								
Unit	Bus	S_{pr} (MW)	I_s (W/m^2)	R_c	μ	σ		
1	5	25	800	120	6	0.6		
2	13	30	800	200	6	0.6		
3	24	30	800	170	6	0.6		
Solar systems connected to the proposed Modified (2) network.								
1	5	25	800	120	6	0.6		
2	13	30	800	200	6	0.6		
3	17	30	800	170	6	0.6		

Table 3: The gas emission and fuel operational cost coefficients of thermal units in the proposed IEEE-30 bus system.

gas emission coefficients				
Generator	bus	α	β	γ
1	1	4.091	-5.554	6.49
2	2	2.543	-6.047	5.638
3	5	4.258	-5.094	4.586
4	8	5.326	-3.55	3.38
5	11	4.258	-5.094	4.586
6	13	6.131	-5.555	5.151
fuel cost coefficients				
Generator	bus	λ	δ	φ
1	1	0	2	0.00375
2	2	0	1.75	0.0175
3	5	0	3	0.025
4	8	0	3.25	0.00834
5	11	0	3	0.025
6	13	0	3	0.025

Table 4: The main parameters value and the parameters testing ranges of the proposed optimization approaches.

Algorithm	Parameters	Values	Testing Range
IPSO [33]	Coefficient of inertia	Decreasing from 0.9 to 0.4 (linearly)	----
	Search agents number	50	25-100
	Maximum iteration number	100	50-200
	Coefficient of acceleration	1 and 2	
ALO [34]	Size of population	50	25-100
	Maximum iteration number	100	50-200
SDO [32]	Size of population	50	25-100
	Maximum iteration number	100	50-200
MFO [35]	Size of population	50	25-100
	Maximum iteration number	100	50-200
	Shape constant	1	0-2
AGPSO [33]	Coefficient of inertia	Decreasing from 0.9 to 0.4 (linearly)	----
	Number of search agents	50	25-100
	Maximum iteration number	100	50-200
	Inertia coefficient	1 and 2	
MRFO [28]	Search agents number	50	25-100
	Initial gravitational constant	100	50-150
	Size of population	50	25-100
	Maximum iteration number	100	50-200
	Somesault factor	2	1-3
CGSA [31]	Chaoatic map	Defined by logistic in [31]	---
	Maximum number of iterations	100	50-200
	Descending coefficient	10	5-15

4.2 Single and multi-objective function results

This section aims to present the IEEE 30-bus model results, which were obtained using the proposed recent heuristic optimization algorithms for all objective function cases, as summarized in Table 1. The objective function values are used to compare the results, where the transmission line loss, emission index, fuel cost and

voltage deviation are given in MW, ton/h, $/h and p.u, respectively. In Table 5, the result showed that the MRFO algorithm outperform all other heuristic optimization algorithms for the given data by achieving the minimum cost function value over all cases. For example, the MRFO has obtained 3.181063 MW in case 1 compared to 4.765994 MW and 3.928019 MW for ALO and CGSA, respectively. However, MRFO and IPSO have obtained close results to case 2, which are 0.204224 ton/h, 0.204987 ton/h, respectively. For case 4, the MRFO and AGPSO have achieved 0.1233304 p.u and 0.1248445 p.u, respectively. The multi-objective function cases (Case 5-7) results showed that MRFO has outperformed other heuristic optimization algorithms in terms of decreasing the objective function values. The transmission line loss, emission index, fuel cost and voltage deviation, as expected, depending on the objective minimized and it has minimum values when individually minimized.

Table 5: Results of the MRFO and the proposed metaheuristic algorithms for IEEE 30-bus model over different objective function cases.

	Case 1	Case 2	Case 3	Case 4	Case 5	Case 6	Case 7
CGSA	3.928019	0.214162	843.8661	0.1311433	857.4699	1073.843	994.36722
SDO	3.620135	0.208335	842.4642	0.1314178	857.0143	1060.094	995.89322
MRFO	3.181063	0.204224	837.8103	0.1233304	853.7259	1059.013	990.01329
IPSO	3.452462	0.204987	841.1485	0.1391369	858.4031	1061.669	995.91718
ALO	4.765994	0.212901	856.3358	0.1367593	859.1723	1071.952	998.95404
MFO	3.395259	0.209613	841.962	0.1285336	858.1296	1061.407	997.81549
AGPSO	3.684243	0.209609	842.6436	0.1248445	858.6297	1060.663	994.29724

The convergence curves presented the relationship between the number of iterations and optimum cost function. For example, Figure 2 illustrated the convergence curves over cases 2 and 7 for all the proposed optimization algorithms. The MRFO algorithm has smoother and speedy convergence curve, where the MRFO has achieved the optimal results within less iterations compared to other metaheuristic optimization approaches, as seen in Figures 3. This showed that the MRFO algorithm has lower computational cost and higher efficiency in CPU utilization.

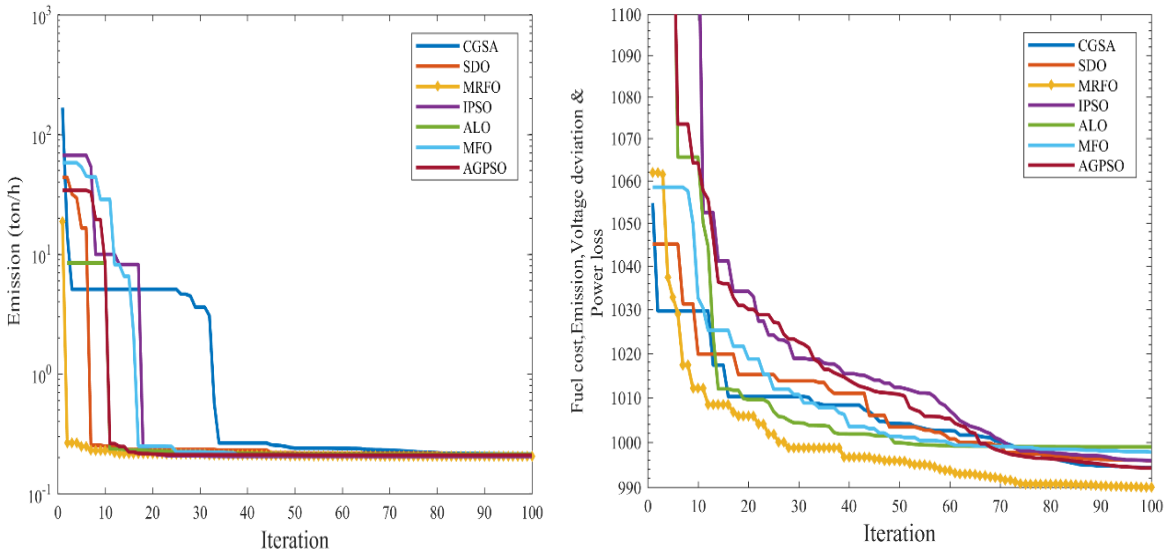

(a) (b)

Fig. 3. Convergence curves of the MRFO and the proposed metaheuristic optimization models for (a) case 2 and (b) case 7.

The previous results showed that the MRFO model outperforms other optimization algorthims and has the minimum objective function values for all cases without any infringement to the limitations and constraints. Table 6 presents the MRFO model results for IEEE 30-bus network for case 1 as an example. In Table 6 and tables in

the Appendix section, the PG is the generators active power, VG is the generator voltage magnitude, QG is the reactive power of generator, QC is the magnitude of shunt capacitor, TS is the tap changer voltage, and VD is the voltage deviation. In Table 6 and all tables in the appendix, the control variables are highlighted as ***bold text*** and state variables as normal text.

Table 6: Results of the MRFO algorithms for IEEE 30-bus model over different objective function cases.

Parameters	Min	Max	case 1	case 2	case 3	case 4	case 5	case 6	case 7
PG1 (MW)	50	200	52.45123	64.52673	139.9879	135.7245	139.8683	95.81943	118.6466
PG2 (MW)	20	80	79.52508	68.26401	58.95586	54.72236	59.21454	53.58874	52.35471
PG5 (MW)	15	50	49.89869	49.98748	20.985	32.99517	24.7227	47.77595	36.22531
PG8 (MW)	10	35	34.92556	34.48852	34.16928	12.89263	30.73691	34.89481	34.8718
PG11 (MW)	10	30	29.86572	29.96472	17.20179	26.22522	18.05257	29.5956	26.84233
PG13 (MW)	10	40	39.9148	39.9716	19.14378	27.872	18.23371	25.73785	19.74797
VG1 (p.u.)	0.95	1.1	1.059105	1.064265	1.074382	1.028337	1.04667	1.065443	1.071
VG2 (p.u.)	0.95	1.1	1.053028	1.054884	1.058575	1.016385	1.027091	1.054636	1.059597
VG5 (p.u.)	0.95	1.1	1.031529	1.034532	1.02783	0.998324	1.004804	1.037331	1.032443
VG8 (p.u.)	0.95	1.1	1.040915	1.024281	1.040362	1.000625	1.004433	1.040804	1.040823
VG11 (p.u.)	0.95	1.1	1.076003	1.076201	1.063444	1.045407	1.009391	1.08264	1.052561
VG13 (p.u.)	0.95	1.1	1.047012	0.968038	1.044096	1.013123	1.004894	1.059065	1.016396
QG1 (MVAr)	-20	150	-2.54692	9.85596	0.245012	-9.38369	11.56811	-2.73418	-4.36391
QG2 (MVAr)	-20	60	3.017738	19.28971	12.03046	10.62814	8.971878	3.680779	17.36502
QG5 (MVAr)	-15	62.5	19.33753	28.90979	23.4239	31.34045	35.10225	24.50257	21.24103
QG8 (MVAr)	-15	48	29.49256	22.39821	32.10829	35.54928	38.44545	25.20361	27.70747
QC10 (MVAr)	0	5	1.608274	1.098943	2.227006	3.824171	3.220963	2.956771	1.435408
QG11 (MVAr)	-10	40	15.17821	23.6746	13.92861	19.46254	1.665713	18.18019	19.76257
QC12 (MVAr)	0	5	4.31586	2.213457	1.445433	1.335555	4.093917	0.888182	1.98635
QG13 (MVAr)	-15	44	12.55374	-13.1849	8.352941	2.628981	-4.13535	9.34424	2.010326
QC15 (MVAr)	0	5	3.497263	2.839656	3.615316	4.599411	2.664672	2.48676	4.479763
QC17 (MVAr)	0	5	4.750872	3.330972	3.882472	2.688204	2.575065	3.814932	4.566432
QC20 (MVAr)	0	5	2.637549	4.460008	4.767304	4.942899	4.518492	3.840383	3.816575
QC21 (MVAr)	0	5	4.881207	1.47523	3.451327	4.709096	2.098408	4.367202	3.145302
QC23 (MVAr)	0	5	1.564046	1.373651	4.787802	4.680784	4.828105	2.709757	3.544914
QC24 (MVAr)	0	5	3.469463	2.386178	2.836615	4.385637	4.921799	4.805279	4.434736
QC29 (MVAr)	0	5	2.497439	1.542376	1.290046	1.665862	3.2387	3.078047	3.069847
TS11 (p.u.)	0.9	1.1	0.976077	0.993108	0.998793	1.028328	1.000398	1.012009	1.052721
TS12 (p.u.)	0.9	1.1	1.05516	0.958774	1.052066	0.936642	0.909349	0.972617	0.984844
TS15 (p.u.)	0.9	1.1	1.027278	1.006784	1.004566	0.98529	0.972054	0.99584	1.014613
TS36 (p.u.)	0.9	1.1	0.988176	1.014805	0.964133	0.955172	0.967209	0.980792	1.006176
VD (p.u.)			0.534452	0.495975	0.578668	0.12333	0.129428	0.858611	0.323022
Fuel cost ($/h)			972.1568	952.3171	837.8103	857.0938	840.6257	898.5184	862.1618
Power line loss (MW)			3.181063	3.803056	7.043596	7.031943	7.428731	4.012376	5.288765
Emission index(ton/h)			0.207202	0.204224	0.28493	0.271953	0.283905	0.222343	0.248169
Objective function			3.181063	0.204224	837.8103	0.12333	853.7259	1059.013	990.0133

4.3 Renewable energy sources (RES) scenarios results

To investigate the impact of incorporating RES to the electrical networks, and the RES locations on the OPF solvers, the IEEE 30-bus model has been adopted in this paper by inserting RES in two different locations, as presented in Section 4.1 The proposed MRFO is compared to the proposed metaheuristic approaches by using Modified (1) and Modified (2) networks. In this section, the MRFO is employed to achieve and find the best optimal solution for OPF problems of electrical networks equipped with RES. The MRFO results of all cases for all power network scenarios are presented in Table 7. These results indicate that the RES and the location of the wind and PV systems have a direct impact on the OPF solutions. In addition, the results showed that the MRFO is an effective solver for the OPF problems with RES. As an example, the objective functions values for case 1 and 3 were decreased from 3.181063 MW and 837.8103 $/h to 2.09218 MW and 0.09114 $/h, respectively, after inserting the RES (Modified (1) network model). By adding the RES to the power network as a negative load value, the total network demand will decreased, which leads to a decline in the transmission losses and fuel operational cost. In turn, the total objective functions for cases 5, 6, and 7 will decrease. Table 7 shows that the maximum reduction in the objective function was 55% in case 2 for Modified (1) and Modified (2) networks. The minimum improvement for adding the RES was equal to 7.7% and 3.9% in case 3 for Modified (1) and Modified (2) networks, respectively. On the other hand, the Modified (1) and Modified (2) networks have displayed close results to cases 2 and 6. This indicates that the location of RES on the power network has a limited impact on the MRFO algorithm in these cases. The MRFO results for Modified (2) system have increased compared to Modified (1) system for case 1 and 7 by around 13% and 16%, respectively.

Table 7: Results of the MRFO algorithm for IEEE 30-bus, Modified (1) and Modified (2) networks for all cases.

	case 1	**case 2**	**case 3**	**case 4**	**case 5**	**case 6**	**case 7**
IEEE 30-bus system	3.181063	0.204224	837.8103	0.12333	853.7259	1059.013	990.0133
IEEE 30-bus Modified (1)	2.09218	0.09114	772.9864	0.074447	795.9037	938.1911	749.9863
IEEE 30-bus Modified (2)	2.409543	0.091077	804.9323	0.083975	788.6009	953.8583	895.2246
The percentage of cost function reduction							
Modified (1) over IEEE 30-bus (%)	34.23017	55.59008	7.737291	39.6359	6.77292	11.40895	11.63351
Modified (2) over IEEE 30-bus (%)	24.25353	55.62086	3.924274	31.91039	7.628322	9.929536	7.804434
Modified (1) over Modified (2) (%)	13.1711	-0.069	3.9688	11.3461	-0.926	1.6425	16.31286

The MRFO results are compared among the proposed recent heuristic optimization algorithms for the Modified (1) and Modified (2) networks over different cases, as presented in Table 8. The optimization algorithms results show that the MRFO is more effective than other heuristic optimization algorithms in solving the OPF problems for electrical networks incorporating RES. For example, Table 8 shows that the MRFO obtained a better result complex multi-objective function with conflict cost functions (case 7) with objective function equal to 749.9863 compared to 802.8756 and 803.41164 for AGPSO and ALO algorithms, respectively. The results in Table 8

indicates that the results of Modified (2) system has been increased compared to Modified (1) system for almost all algorithms.

Table 8: Results of the proposed optimization algorithms results for Modified (1) and Modified (2) networks for case 7.

	AGPSO	**MFO**	**ALO**	**IPSO**	**MRFO**	**SDO**	**CGSA**
IEEE 30-bus Modified (1)	802.8756	772.94109	803.41164	769.07981	**749.9863**	773.84641	771.07042
IEEE 30-bus Modified (2)	901.6399	933.80365	901.89125	944.26979	**895.2246**	916.38100	928.6616

In Figure 4, the impact of the renewable energy sources on the total generation costs by using different OPF solvers is presented. Generally, the MRFO outperformed all other algorithms by achieving the minimum costs for the IEEE 30-bus without renewable energy resources (fed by the utility) and Modified (1) network with renewable energy resources. In the power networks Modified (1) with renewable energy sources, the total generation costs for all solvers decreased compared to the IEEE 30-bus without renewable energy resources. This indicates that the renewable energy resources locations has a significant impact on reducing the generation costs. For example, the MRFO recorded the maximum improvement with cost reduction equal to 11%, whereas the minimum reduction in total generation cost was 5% for IPSO algorithm.

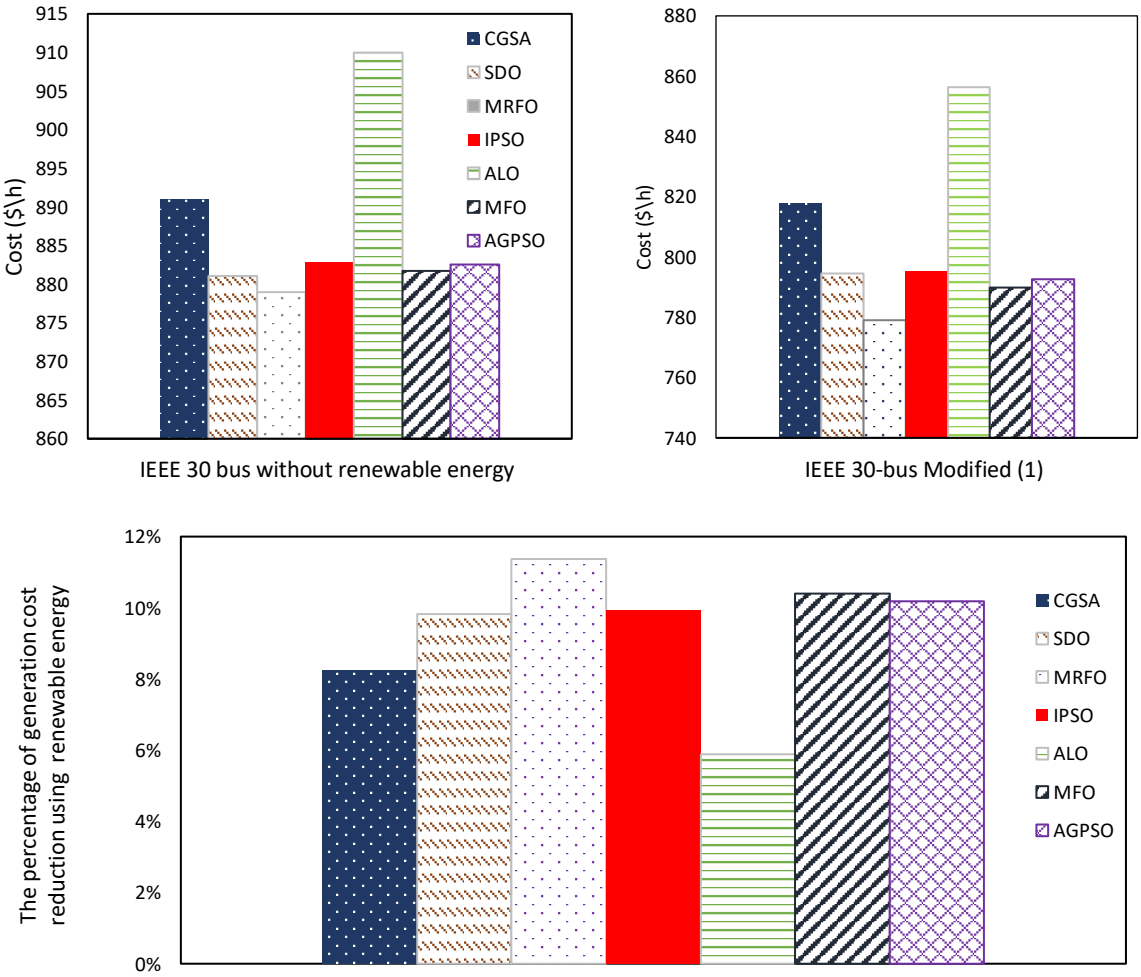

Fig. 4. The total generation costs for the IEEE 30-bus without renewable energy resources (fed by utility) and Modified (1) network with renewable energy resources and percentage of generation cost saving.

4.4 Increase in demand and power line outgas results

The electricity demand is significantly growing every year due to the shifting towards electrification of transport, increasing electricity usage level at homes due to using electricity loads such as heating and air conditioning and growing population. This will increase the pressure on the power network infrastructure and energy suppliers. Nowadays, one of the main challenges that face distribution network operators increase in electricity demand, which may lead to outage and failure to cover the required load demand. To examine the impact of these conditions on the optimization algorithm performance, the proposed MRFO algorithm is tested on the three networks (IEEE 30-bus, Modified (1) and Modified (2) networks) with 30% load increase and line outages on the power network, as presented in Table 8. Then, a comparison analysis for the impact of increasing the electrical demand and power system outages for the MRFO and the other heuristic optimization algorithms is presented in Table 9. In this section, the power system outage was for transmission lines (2 to 6) and (10 to 21), which presented the main power lines close to the generator units.

The results in Table 9 indicate that the increase in the electrical demand and network outages conditions has a significant impact on the OPF solutions. As an example, the objective function values for case 1 and 7 were dramatically increased from 3.18106 MW and 990.01 for IEEE 30-bus system to 10.3562 MW and 1460.03, respectively, after increasing the demand by 30% and having number of line outages. In addition, the results show that by adding the RES to the power network (Modified (1) and Modified (2) networks), the impact of the power network outages and the increase in demand is less compared to networks without RES (IEEE 30-bus network). For example, Table 9 shows that the emission index function (Case 2) increased by 40.5%, 16.4% and 15.9% for Modified (1) and Modified (2) networks, respectively, after increasing the demand and the line outages. Furthermore, the results indicate that the location of RES on the power network has a limited impact on the MRFO algorithm, where, the Modified (1) and Modified (2) systems have shown close result for all cases. The details MRFO results for all network scenarios have been shown in Appendix A, Tables A1–A5.

Table 9: Results of the MRFO algorithm for different power network systems under increasing demand and transmission line outages conditions

	case 1	**case 2**	**case 3**	**case 4**	**case 5**	**case 6**	**case 7**
IEEE 30-bus network	3.18106	0.20422	837.810	0.12333	853.725	1059.013	990.01
IEEE 30-bus modified -1	2.09218	0.09114	772.986	0.07444	795.903	938.1911	749.986
IEEE 30-bus modified- 2	2.40954	0.09107	804.932	0.08397	788.600	953.8583	895.224
IEEE 30-bus network with 30% increase in load and outages of some transmission lines	10.3562	0.28707	1167.435	0.20311	1193.317	1633.216	1460.03
IEEE 30-bus modified 1 with 30% increase in load and outages of some transmission lines	5.36663	0.10612	1072.905	0.08613	1077.842	1360.785	1249.93
IEEE 30-bus modified 2 with 30% increase in load and outages of some transmission lines	7.30354	0.10562	1052.049	0.14091	1123.534	1382.903	1286.25

Table 10 presents the MRFO algorithm results compared among the proposed recent heuristic optimization algorithms for single objective function problem (case 1) and multi-objective function (case 7) for the Modified (1) and Modified (2) networks after increasing the load demand and having outage on the power network. These

results demonstrate that the MRFO algorithm is more effective than other metaheuristic optimization approaches in solving the OPF problems under abnormal conditions. For example, the MRFO displayed a better result for case 3 for Modified (1) network with 30% increase in load and outages of some transmission lines with objective function equal to 1072.952 $/h compared to 1105.9788 $/h and 1104.973 $/h for AGPSO and CGSA algorithms, respectively. As demonstrated in the previous section, changing the location of the RES does not have a direct impact on the optimization algorithm results and performance.

Table 10: Results of the proposed optimization algorithms results for Modified (1) and Modified (2) networks considering 30% load increasing and line outages.

	AGPSO	**MFO**	**ALO**	**IPSO**	**MRFO**	**SDO**	**CGSA**
				Case 3			
IEEE 30-bus Modified (1)	1105.9788	1079.3829	1078.4191	1112.2389	**1072.9052**	1073.3601	1104.973
IEEE 30-bus Modified (2)	1089.0076	1077.3109	1065.3384	1074.3852	**1052.0499**	1086.0282	1072.918
				Case 7			
IEEE 30-bus Modified (1)	1293.3283	1295.0288	1295.7599	1332.3993	**1249.935**	1294.1581	1354.741
IEEE 30-bus Modified (2)	1322.8860	1293.8097	1307.5417	1347.9242	**1286.251**	1308.5756	1333.435

4.5 Statistical analysis for the MRFO and the proposed metaheuristic optimization algorithms

In the previous sections, the MRFO algorithm outperformed the other heuristic optimization methods and and proved to be the most effective solver for all network model scenarios. In order to provide a further evidence on the performance of MRFO, the proposed metaheuristic optimization approaches in this article were used to solve case 1 problem over 1000 runs of simulations. The statistical analysis for the proposed optimization algorithm is presented in Table 11 including the minimum and maximum cost function values over the 30 runs for all methods. Furthermore, the median and standard deviation values for the cost function over the 30 runs for all methods is presented in Table 11. The results show that the MRFO is the most effective solver compared to other heuristics methods because it achieved lower cost function values for the minimum, maximum, median values and standard deviation. For example, the standard deviation for the MRFO had a lower compared to the other metaheuristic optimization techniques with values equal to 0.0392.

Table 11: Statistical analysis for the proposed optimization method over case 1.

	Minimum	**Maximum**	**Median**	**Standard deviation**
AGPSO	3.684242972	4.0789175	3.74279579	0.148931363
MFO	3.39525918	3.60128064	3.469399978	0.067816401
ALO	4.765994381	6.038091104	5.362548392	0.460612714
IPSO	3.452462153	4.30687017	3.498564623	0.272798974
MRFO	3.181063492	3.332614406	3.276390137	0.039221242
SDO	3.62013511	4.139257779	3.836721806	0.147978987
CGSA	3.928019042	4.963097807	4.435250265	0.314260995

4.6 Estimate of computational costs

The average of computational cost (execution time) for solving the OPF problems (Cases 1 to 7) for IEEE 30-bus system is presented in Figure 5 for different optimization techniques. This approximation of computational cost has been made on 2.8-GHz i7 PC with 16 GB of RAM. To check the computational cost of each algorithm, 100 independent trials are performed and the average of the results is shown in this section. In general, the MRFO, IPSO and AGPSO recorded the lower execution time around 11 s for all cases, while the CGSA, SDO and ALO algorithms reordered more than 20 s for all cases. The MRFO outperformed all other algorithms and achieved the lowest computational cost for all cases. This is mainly due to the fact that the MRFO algorithm requires a few numbers of parameters which makes it an easily implementable and promising algorithm for engineering applications.

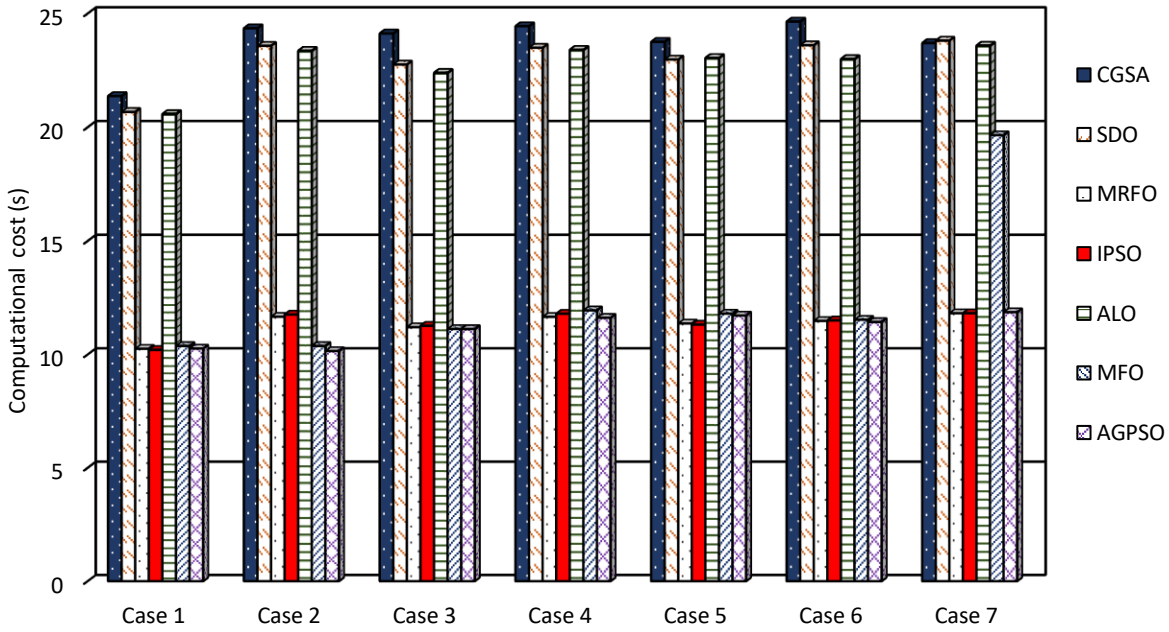

Fig. 5. The computational cost of the MRFO and the other metaheuristic optimization technique for IEEE 30-bus system over all cases.

4.7 Analysis of exploration and exploitation performance in MRFO algorithm

In general, the exploration behavior in MRFO aims to look for the optimal solution within a wide variable space. The exploration search in areas are not neighbor to the current position (solution), which let the exploration process be more extensive and random process as possible but it helps the algorithm to avoid local optimal solutions [28]. The exploitation behavior in MRFO works on confining the search process into a small region from the exploration process. The exploitation search on the promising region from the searching space at exploration. In MRFO, at each iteration, t, the position of each individual in the domain will be updated based on the current searching position and reference position. The value of the ratio between the current iteration, t, and maximum iterations number (T) decreases from (1/T) to 1 which means moving from exploratory to exploitative search, respectively [28]. In this section, the exploration and exploitation performance presented for the IEEE 30-bus model with Case 1 (power transmission loss). Figure 6 presented the convergence curves for the exploration and exploitation process over Cases 1. The convergence curve of exploration process showed a low performance at iterations less than 10 compared to the exploitation process where the exploration search within larger space at

the beginning of the searching process. However, both exploration and exploitation process showed similar convergence behavior after the iteration number 15 as the searching space became more specific.

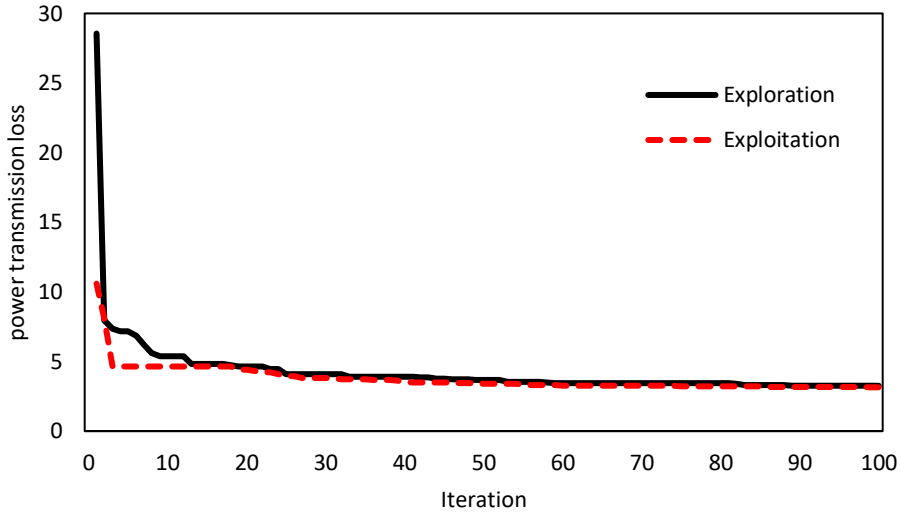

Fig. 6. Convergence curves of the exploration and exploitation process in MRFO algorithm for IEEE 30-bus system (Case 1).

4.8 Largescale system results

To examine the scalability of the proposed MRFO algorithm, an IEEE 118-bus power network is employed as large-scale power network model. The data and network specification of IEEE 118-bus system are extracted from [3,39]. The IEEE 118-bus system has 54 thermal power generation units, 118 buses, 130 branches and the swing bus is chosen to be bus 65. The voltage magnitude limits are 0.95–1.06 p.u for the load and generators. Furthermore, the tap changer setting is 0.9-1.1 p.u. Moreover, the limit of the voltage automatic regulator compensators is 0 - 0.3 p.u. The active and reactive demand values , in this system, equal 2.834 p.u and 1.262 p.u, respectively, and the total load is 100 MVA. The proposed MRFO and other heuristics optimization approaches are employed to solve OPF problem in case 3, minimizing the fuel operational cost, as presented in Table A.6. The results in Table 12 show that the MRFO displayed a better result and outperformed other heuristic optimization methods and is more effective in solving and handling OPF problems for large-scale network. For example, the MRFO achieved an objective function for case 3 equal to 135606.4538 $/h compared to 146423.6197 $/h and 139380.565 $/h for AGPSO and IPSO, respectively.

Table 12: Results of the proposed optimization algorithms results for IEEE 118-bus network (case 3).

Optimization algorithm	**Objective function ($/h)**
AGPSO	146423.619
MFO	136484.918
IPSO	139380.595
MRFO	**135606.453**
SDO	136708.054
ALO	136122.470
CGSA	140243.971

As a large-scale system, it is interesting to check the convergence rate for all optimization methods. Figure 7 presents the convergence curves over case 3 for all the proposed optimization algorithms. The MRFO algorithm has smoother and speedy convergence curve, and it achieved the optimal results within 300 iterations compared to other heuristic optimization algorithms, as seen in Figure 7. However, ALO algorithm displayed a close result for number of iterations under 300 but the curve was not smooth. This indicates that the MRFO algorithm has lower computational cost and higher efficiency in CPU utilization.

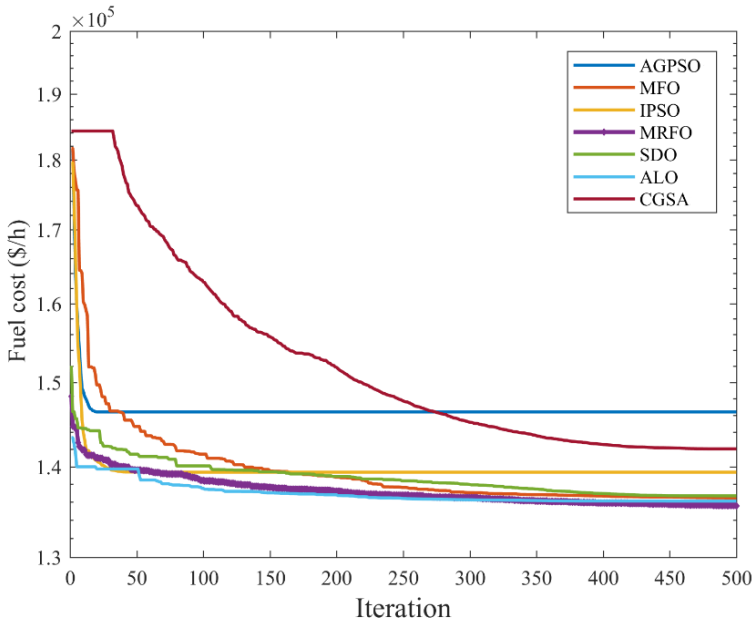

Fig. 7. Convergence curves of the MRFO and the other metaheuristic optimization technique for IEEE 118-bus system.

The computational cost (execution time) for solving the OPF problem (Cases 3) for the IEEE 118-bus system is presented in Table 13 for the proposed optimization techniques. Generally, the computational cost results of all algorithms for the IEEE 118-bus system increased compared to IEEE 30-bus system. The execution time increased from simulations in up to 24 s. (IEEE 30-bus) to 34 min. (IEEE 118-bus) due to the high complexity and high number of parameters of the IEEE-118 bus model. However, the CGSA, MRFO, IPSO, MFO and AGPSO recorded the lower execution time around 17.54, 17.57, 16.73, 16.29 and 16.20 min, respectively, for the IEEE 118-bus system (Case 3). While the SDO and ALO algorithms reordered more than half hour with 33.98 and 30.37 min, respectively. This approximation of computational cost has been made on 2.8-GHz i7 PC with 16 GB of RAM. The showed the algorithms which required a few numbers of parameters such as MRFO are more easy to implement and promising algorithm for engineering applications

Table 13: Results of the computational cost for the proposed optimization algorithms results for IEEE 118-bus network (case 3).

Optimization algorithm	**Computational cost (minutes)**
AGPSO	16.20895
MFO	16.2908
IPSO	16.73787
MRFO	17.57983
SDO	33.98215
ALO	30.37941
CGSA	17.54448

4.9 Discussion

An optimal power management solution has become a significant tool to develop cost effective and environmentally friendly power supply network. Since there is limited research on using metaheuristic algorithms on OPF problems. Therefore, this article introduced a novel optimization algorithm inspired by the vitality, namely: Manta Ray Foraging Optimization (MRFO), to figure out both multi and single objective problems of Optimal Power Flow (OPF) incorporating stochastic RES. In addtion, the new MRFO algorithm and some modern metaheuristic algorithms were used and compared to settle the issue of OPF, enhance the energy efficiency, environment and cost performance of the power network. The proposed algorithms are tested with bus systems as 30 and 118 and outcome from the suggested MRFO is compared to six metaheuristic optimization algorithms (CGSA, SDO, IPSO, ALO, MFO and AGPSO). Moreover, OPF challenges are successfully settled by the MRFO algorithm and outperform the proposed metaheuristic optimization methods. The MRFO algorithm outperformed all other optimization algorithms for the given data by achieving the minimum cost function value over all cases. For example, the MRFO has obtained 3.181063 MW in case 1 compared to 4.765994 MW and 3.928019 MW for ALO and CGSA, respectively. By adding the RES to the power network, which leads to a decline in the transmission losses and fuel operational cost. The MRFO results for Modified (2) system have increased compared to Modified (1) system for case 1 and 7 by around 13% and 16%, respectively. Finally, in term of the computational cost, the MRFO outperformed all other algorithms and achieved the lowest computational cost for all cases. This is mainly due to the fact that the MRFO algorithm requires a few numbers of parameters which makes it an easily implementable and promising optimization algorithm for engineering applications.

In order to examine the performance of MRFO compared to literature, the Differential Evolution (DE) algorithm [41] is employed in this section to solve the OPF problems. The DE algorithm is one of the common heuristic optimization algorithms, where it easy to implement and fast. However, the DE is highly sensitive to the choosing of the mutation strategy. Table 14 presented the results of the MRFO and DE algorithms for IEEE 30-bus model over different objective function cases. In Table 13, the result showed that the MRFO algorithm outperform the DE algorithm for the given data by achieving the minimum cost function value over all cases. For example, the MRFO has obtained 3.181063 MW in Case 1 compared to 4.22558 MW for DE. However. For case 4, the MRFO has achieved 0.1233304 p.u compared to 0.129344 p.u for DE algorithm. The multi-objective function cases (Case 5-7) results showed that MRFO has outperformed DE in terms of decreasing the objective function values.

Table 14: Results of the MRFO and DE algorithms for IEEE 30-bus model over different objective function cases.

	MRFO	**DE**
Cas 1	3.181063	4.22558
Cas 2	0.204224	0.205291
Cas 3	837.8103	846.7418
Cas 4	0.1233304	0.129344
Cas 5	853.7259	859.302
Cas 6	1059.013	1079.569
Cas 7	990.01329	1004.946

5. Conclusions

In this work, a new MRFO algorithm has been employed to find the best optimal solution of different OPF problems for two electrcial network systems, IEEE 30-bus and 118-bus networks, equipped with RES. The OPF problems have been formulated based on single and multi-objective functions through seven cases considering the transmission line loss, emission index, fuel operational cost and voltage level deviation. To present the volatile nature of RES, the power network included a realistic RES model (wind and solar systems) based on probabilistic estimation model. This paper aims to provide a new optimal controller able to handle the RES and distribution network load nature compared to conventional optimization methods. In the results section, the MRFO have been tested and evaluated compared to six recent metaheuristic optimization techniques, namely: CGSA [31], SDO [32], IPSO [33], ALO [34], MFO [35], AGPSO [33].The MRFO model outperformed all other metaheuristic optimization techniques for IEEE network scenarios without and with RES in different locations. Recent and new heuristics optimization algorithms have been used and compared in this paper to provide the decision maker different suitable optimization techniques. The implementation of the recent metaheuristic algorithms presented in this article and installing an energy storage system to the distribution network is part of our future work.

References

1. Biswas P, Suganthan N, Qu Y, Amaratunga A. Multiobjective economic-environmental power dispatch with stochastic wind-solar-small hydro power. *Energy* 2018, 150, 1039–1057.
2. Alomoush M. Microgrid combined power-heat economic-emission dispatch considering stochastic renewable energy resources, power purchase and emission tax. *Energy Conversion and Management* 2019, 200, 103300.
3. Nusair K, Alasali F. Optimal Power Flow Management System for a Power Network with Stochastic Renewable Energy Resources using Golden Ratio Optimization Method. *Energies* 2020, 13, 3671.
4. Shi L,Wang C, Yao L, Ni Y, Bazargan M. Optimal power flow solution incorporating wind power. IEEE Syst. J. 2011, 6, 233–241.
5. Alasali F, Haben S, Holderbaum W. Energy management systems for a network of electrified cranes with energy storage. Int. J. Electr. Power Energy Syst. 2019, 106, 210–222.
6. Roy R, Jadhav H. Optimal power flow solution of power system incorporating stochastic wind power using Gbest guided artificial bee colony algorithm. Int. J. Electr. Power Energy Syst. 2015, 64, 562–578.
7. Lin M, Huang H, Zhan S. A hybrid current-power optimal power flow technique. *IEEE Trans. Power Syst*. 2008, 23, 177–185.
8. Zhong Q, Xue S, Wang Z, Duan J, Zeng M, Zhang G. Environmental and economic dispatch model for smart microgrid based on shuffled frog leap algorithm optimized by random Nelder Mead. *Przeglad Elektrotechniczny* 2013: 147-51.
9. Glavitsch H, Spoerry M. Quadratic loss formula for reactive dispatch. *IEEE Trans. Power Appar*. Syst. 1983, 102, 3850–3858.
10. Elattar E, ElSayed S. Modified harmony search algorithm for combined economic emission dispatch of microgrid incorporating renewable sources. *Energy* 2018;159:496-507.
11. Elattar E. Modified JAYA algorithm for optimal power flow incorporating renewable energy sources considering the cost, emission, power loss and voltage profile improvement. *Energy* 2019;178: 598-609.
12. Burchett R, Happ H. Wirgau, K. Large scale optimal power flow. *IEEE Trans. Power Appar. Syst*. 1982, 10, 3722–3732.
13. Wang X, Chen S, Zhou Y, Wang J, Cui Y. Optimal dispatch of microgrid with combined heat and power system considering environmental cost. *Energies* 2018;11:2493. https://doi.org/10.3390/en11102493.
14. Abido MA. Optimal power flow using particle swarm optimization. *Int J Electr Power Energy Syst* 2002;24:563-571.
15. Dommel, H.; Tinney, W. Optimal Power Flow solutions. IEEE Trans. Power Appar. Syst. 1968, PAS–87, 1866–1876.
16. Taha B, Elattar E. Optimal reactive power resources sizing for power system operations enhancement based on improved grey wolf optimiser. *IET Gener. Transm. Distrib*. 2018, 12, 3421–3434.
17. Nemati M, Braun M, Tenbohlen S. Optimization of unit commitment and economic dispatch in microgrids based on genetic algorithm and mixed integer linear programming. *Appl Energy* 2018;210:944–63. https://doi.org/10.1016/j.apenergy.

18. Hazra J, Sinha A. A multi-objective optimal power flow using particle swarm optimization. Eur. Trans. Electr. Power 2011, 21, 1028–1045.
19. Mohamed A, Mohamed S, El-Gaafary A, Hemeida M. Optimal power flow using moth swarm algorithm. *Electr. Power Syst*. Res. 2017, 142, 190–206.
20. Shilaja C, Arunprasath T. Optimal power flow using Moth Swarm Algorithm with Gravitational Search Algorithm considering wind power. *Future Gener. Comput. Syst*. 2019, 98, 708–715.
21. Aien M, Fotuhi-Firuzabad M, Rashidinejad M. Probabilistic optimal power flow in correlated hybrid wind–photovoltaic power systems. IEEE Trans. *Smart Grid* 2014, 5, 130–138.
22. Aien M, Rashidinejad M, Firuz-Abad F. Probabilistic optimal power flow in correlated hybrid wind-PV power systems: A review and a new approach. Renew. *Sustain. Energy Rev*. 2015, 41, 1437–1446.
23. Bhattacharya A, Roy P. Solution of multi-objective optimal power flow using gravitational search algorithm. *IET Gener. Transm. Distrib* 2012, 6, 751–763.
24. Kumar S, Chaturvedi D. Optimal power flow solution using fuzzy evolutionary and swarm optimization. *Int. J. Electr. Power Energy Syst.* 2013, 47, 416–423.
25. Pietrosanti S, Alasali F, Holderbaum W. Power Management System for RTG Crane Using Fuzzy Logic Controller. *Sustainable Energy Technologies and Assessments* 2020, vol. 37, 100639.
26. Liang H, Tsai R, Chen T, Tseng T. Optimal power flow by a fuzzy based hybrid particle swarm optimization approach. *Electr. Power Syst. Res*. 2011, 81, 1466–1474.
27. Khorsandi A, Hosseinian S, Ghazanfari A. Modified artificial bee colony algorithm based on fuzzy multi-objective technique for optimal power flow problem. *Electr. Power Syst. Res*. 2013, 95, 206–213.
28. Zhao W, Zhang Z, Wang L. Manta ray foraging optimization: An effective bio-inspired optimizer for engineering applications. *Engineering Applications of Artificial Intelligence* 2020, 87, 103300
29. Hu F, Hughes J, Ingham B, Ma L, Pourkashanian M. Dynamic economic and emission dispatch model considering wind power under Energy Market Reform: A case study. *Int. J. Electr. Power Energy Syst*. 2019, 110, 184–196.
30. Biswas.P, Suganthan N, Mallipeddi R, Amaratunga A. Optimal reactive power dispatch with uncertainties in load demand and renewable energy sources adopting scenario-based approach. *Appl. Soft Comput*. 2019, 75, 616–632.
31. Mirjalili S, Gandomi H. Chaotic gravitational constants for the gravitational search algorithm. *Applied soft computing*, 2017,53, 407-419.
32. Zhao W, Wang L, Zhang Z. Supply-demand-based optimization: a novel economics-inspired algorithm for global optimization. *IEEE Access* 2019, 7, 182- 206.
33. Mirjalili S, Lewis A, Sadiq A. Autonomous particles groups for particle swarm optimization. *Arabian Journal for Science and Engineering* 2014, 39, 4683-4697.
34. Mirjalili S. The Ant Lion Optimizer. *Advances in Engineering Software* 2015, 83, 80-98.
35. Zhao W, Zhang Z, Wang L.Manta ray foraging optimization: An effective bio-inspired optimizer for engineering applications. *Engineering Applications of Artifcial Intelligence* 2020, 87, 103300.
36. Biswas, P.; Arora, P.; Mallipeddi, R.; Suganthan, P.; Panigrahi, B. Optimal placement and sizing of FACTS devices for optimal power flow in a wind power integrated electrical network. *Neural Computing and Applications*, 2020, https://doi.org/10.1007/s00521-020-05453-x.
37. Nusair, K.; Alasali, F.; Hayajneh, A.; Holderbaum, W. Optimal placement of FACTS devices and power-flow solutions for a power network system integrated with stochastic renewable energy resources using new metaheuristic optimization techniques. *International Journal of Energy Research*, 2021, DOI: 10.1002/er.6997
38. Taha B, Elattar, E. Optimal reactive power resources sizing for power system operations enhancement based on improved grey wolf optimiser. *IET Gener. Transm. Distrib*. 2018, 12, 3421–3434.
39. Alsac O, Stott B. Optimal load flow with steady-state security. *IEEE Trans. Power Appar. Syst.* 1974, 3, 745–751.
40. Zimmerman D, Murillo-Sánchez E, Gan D. MATPOWER: A MATLAB Power System Simulation Package; Manual, Power Systems Engineering Research Center: Ithaca, NY, USA, 1997; Volume 1.
41. Mallipeddi, R.; Suganthan, P.; Pan, Q.; Tasgetiren, M. Differential evolution algorithm with ensemble of parameters and mutation strategies. *Applied Soft Computing, 2011*, 11, pp. 1679-1696.

Appendix A

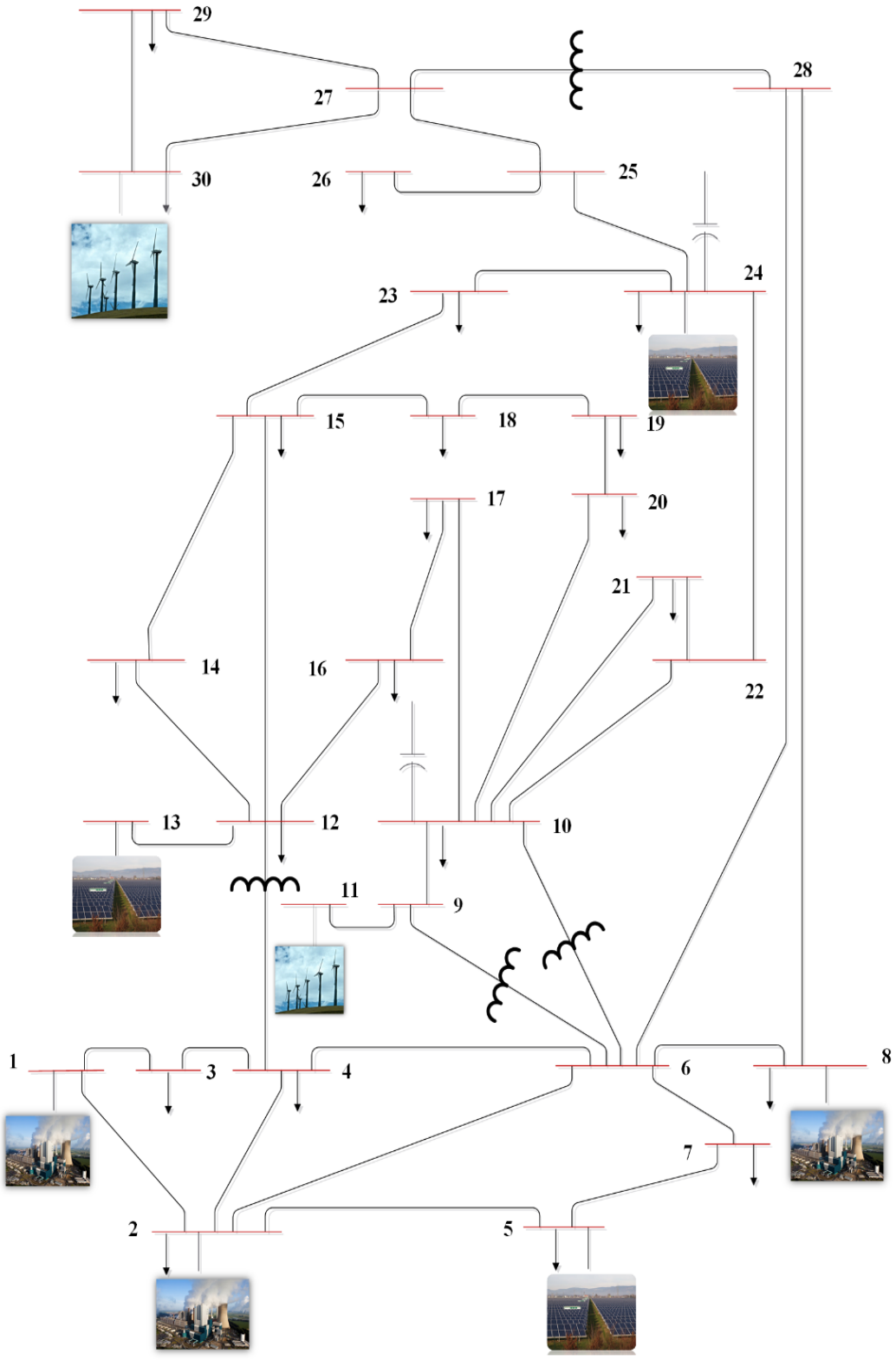

Fig. A.1 IEEE 30-bus Modified (1) network.

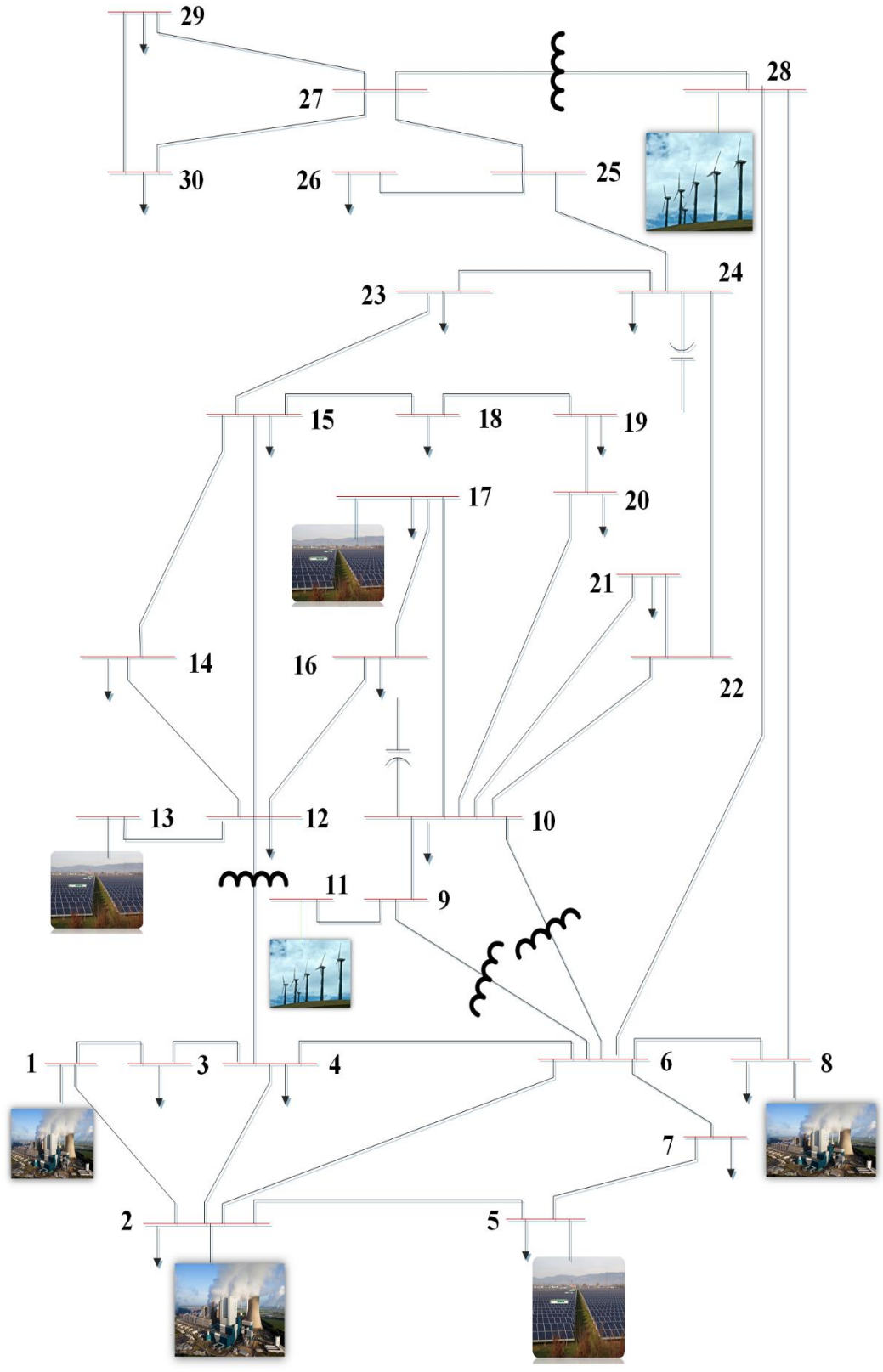

Fig. A.2. IEEE 30-bus Modified (2) network model.

Table A.1: Results of the MRFO algorithms for Modified (1) network model over different objective function cases.

Parameters	Min	Max	case 1	case 2	case 3	case 4	case 5	case 6	case 7
PG2 (MW)	20	80	53.10217	48.07466	32.94601	52.01362	36.43982	54.98197	37.05768
PG5 (MW)	15	50	49.63039	44.81097	23.93882	42.24296	18.12777	44.79729	39.61072
PG8 (MW)	10	35	33.6883	34.18198	15.21964	22.95162	15.68816	30.73283	21.10183
PG11 (MW)	10	30	29.15468	26.46959	22.53192	21.02408	17.71029	21.20181	22.95418
PG13 (MW)	10	40	32.22617	28.37741	25.1366	23.71591	27.36847	28.54333	32.52251
PG24 (MW)	10	30	23.26583	30.35393	20.45652	22.07107	31.18611	22.04507	23.87276
PG30 (MW)	10	40	14.30296	24.64489	19.82092	19.81776	19.85457	13.57662	18.27899
V1 (p.u.)	0.95	1.1	1.042974	1.043735	1.029566	1.023102	1.059126	1.056807	1.048096
V2 (p.u.)	0.95	1.1	1.037619	1.024446	1.012832	1.021021	1.033664	1.053581	1.036026
V5 (p.u.)	0.95	1.1	1.021754	0.971964	0.982048	1.006501	0.986745	1.026678	1.015858
V8 (p.u.)	0.95	1.1	1.028307	0.985283	0.982123	0.994553	0.990354	1.044738	1.015983
V11 (p.u.)	0.95	1.1	1.017064	0.985269	1.036049	1.038617	0.975677	1.087042	1.030732
V13 (p.u.)	0.95	1.1	1.057979	0.987437	0.987846	0.989488	1.028588	1.031164	1.024036
V24 (p.u.)	0.95	1.1	1.048095	0.982508	0.996259	1.020084	1.013762	1.033888	1.011005
V30 (p.u.)	0.95	1.1	1.047869	1.058702	1.003829	0.994556	1.010163	1.034495	0.999635
QC10 (MVAr)	0	5	2.709669	2.834854	2.878847	3.267427	4.898477	2.44212	1.956199
QC12 (MVAr)	0	5	1.907855	2.22496	1.433953	1.585303	1.334457	3.230505	3.127213
QC15 (MVAr)	0	5	3.236474	1.519369	2.040478	3.3857	2.783895	3.815968	1.641764
QC17 (MVAr)	0	5	3.301172	1.912732	2.161203	3.671866	1.487661	2.049416	2.636066
QC20 (MVAr)	0	5	2.387955	2.262026	2.088197	4.754891	3.885065	2.415719	1.01972
QC21 (MVAr)	0	5	2.230793	3.103763	2.414129	2.051029	1.382453	4.021438	2.275083
QC23 (MVAr)	0	5	1.983756	0.709728	4.162238	2.894224	1.828182	3.412833	3.843702
QC24 (MVAr)	0	5	2.310883	3.633435	1.123758	2.889005	2.60504	3.961491	1.650644
QC29 (MVAr)	0	5	2.194497	3.109543	3.710817	3.490717	2.503892	2.733164	2.054229
T11 (p.u.)	0.9	1.1	0.955064	0.971119	1.017779	1.051917	0.923558	0.994171	1.063002
T12 (p.u.)	0.9	1.1	0.967489	1.034648	0.926286	0.932673	0.9636	1.069785	0.984622
T15 (p.u.)	0.9	1.1	0.992005	0.952204	0.995202	0.944508	1.001144	0.961325	1.021147
T36 (p.u.)	0.9	1.1	0.974354	1.033271	0.941588	0.994846	1.025545	1.021236	1.05964
PG1 (MW)	50	200	50.12168	50.26699	129.454	83.39577	123.3727	70.28122	91.66999
QG1 (MVAr)	-20	150	-3.7992	38.44965	5.180942	-13.8634	30.66366	-12.0001	-0.32295
QG2 (MVAr)	-20	60	9.217485	28.63081	23.18515	30.19853	24.68527	21.1628	6.812256
QG5 (MVAr)	-15	62.5	25.8976	2.7691	27.39866	34.32917	19.52058	14.53575	24.94962
QG8 (MVAr)	-15	48	35.36776	8.544639	19.29343	13.95259	16.12931	30.81041	7.242511
QG11 (MVAr)	-10	40	-10.3333	-0.10446	19.92168	20.12693	-18.7655	20.77132	18.24767
QG13 (MVAr)	-15	44	11.98071	-1.92601	1.548432	-12.5582	12.96609	-6.50249	12.35813
QG24 (MVAr)	-15	44	10.04775	0.309948	6.04246	15.68824	7.396501	3.792129	16.15183
QG 30 (MVAr)	-15	44	-0.01355	12.13142	-6.06147	-4.99356	2.359617	1.596974	1.892531
Objective function			2.09218	0.09114	772.9864	0.074447	795.9037	938.1911	749.986

Table A.2: Results of the MRFO algorithms for Modified (2) network model over different objective function cases.

Parameters	Min	Max	case 1	case 2	case 3	case 4	case 5	case 6	case 7
PG2 (MW)	20	80	41.26976	46.03051	50.21708	42.90434	41.57726	47.50968	51.11793
PG5 (MW)	15	50	49.87673	45.85056	16.38781	42.74314	20.69422	42.6933	31.68752
PG8 (MW)	10	35	34.03808	34.99891	15.94532	27.03659	15.66154	33.02222	27.10051
PG11 (MW)	10	30	26.71325	23.39222	14.42703	29.18163	13.58418	20.092	19.67384
PG13 (MW)	10	40	35.48068	38.06924	24.33229	26.50477	25.96712	32.03786	23.85832
PG24 (MW)	10	30	28.98175	25.62961	22.66975	29.41947	20.46784	23.4189	27.18945
PG30 (MW)	10	40	19.32172	22.92367	24.74107	12.78315	16.54969	17.56075	23.97139
V1 (p.u.)	0.95	1.1	1.05322	1.046666	1.044637	1.016361	1.023397	1.031602	1.035555
V2 (p.u.)	0.95	1.1	1.045335	1.030763	1.023774	1.011042	1.001503	1.02875	1.02933
V5 (p.u.)	0.95	1.1	1.027824	0.971653	0.966154	1.00012	0.985017	1.008071	1.008081
V8 (p.u.)	0.95	1.1	1.041659	1.007847	1.010159	0.997212	0.991726	1.019416	1.010569
V11 (p.u.)	0.95	1.1	1.040673	1.048767	1.054652	1.006254	1.012243	1.042945	1.004422
V13 (p.u.)	0.95	1.1	1.051495	1.013657	1.034143	1.005583	1.044254	1.03366	1.038148
V24 (p.u.)	0.95	1.1	1.024744	1.016531	1.026012	1.018366	1.01503	1.024023	1.016218
V30 (p.u.)	0.95	1.1	1.034548	1.032327	1.062038	1.017632	1.022829	1.028042	1.017985
QC10 (MVAr)	0	5	1.866647	2.882352	1.260363	2.210579	1.065362	2.719868	4.003627
QC12 (MVAr)	0	5	3.232075	0.901549	2.886921	0.938107	1.534628	3.16147	2.521854
QC15 (MVAr)	0	5	3.445747	3.194922	1.545543	4.580346	1.25331	2.59011	3.073014
QC17 (MVAr)	0	5	4.131541	4.905936	0.653646	3.790853	1.274772	0.832628	1.911283
QC20 (MVAr)	0	5	3.308342	0.774057	1.495331	4.789223	4.570564	4.685877	3.649528
QC21 (MVAr)	0	5	3.698954	0.229876	4.106533	2.276768	3.009614	3.519136	1.858349
QC23 (MVAr)	0	5	3.970972	1.785421	3.274069	3.801528	3.350577	1.49005	1.545233
QC24 (MVAr)	0	5	3.37165	2.032923	3.844517	4.576448	2.136412	0.699983	2.261085
QC29 (MVAr)	0	5	3.057844	0.785225	4.145339	3.720081	3.63434	3.325993	3.330121
T11 (p.u.)	0.9	1.1	0.975897	0.944684	1.012401	1.021274	0.991878	0.976485	0.990925
T12 (p.u.)	0.9	1.1	1.063503	1.094021	0.982655	0.937774	0.974741	0.960351	1.027059
T15 (p.u.)	0.9	1.1	1.044673	1.091848	0.913571	0.974064	0.972777	0.9864	1.033247
T36 (p.u.)	0.9	1.1	1.003808	1.046128	1.000571	0.997979	0.999807	1.033053	0.994348
PG1 (MW)	50	200	50.12757	50.1212	121.5146	76.31505	135.8922	70.34842	82.99339
QG1 (MVAr)	-20	150	-2.5168	18.8621	16.46883	-10.4469	8.470261	-14.9524	-11.3586
QG2 (MVAr)	-20	60	-1.23268	15.44455	17.1281	12.78753	-11.6449	19.28501	15.30275
QG5 (MVAr)	-15	62.5	19.78951	-12.4005	-1.22409	33.30156	34.42281	22.88972	28.01875
QG8 (MVAr)	-15	48	28.29284	8.220352	34.56509	21.63146	27.61989	30.47642	16.86162
QG11 (MVAr)	-10	40	2.644352	7.955274	16.24934	3.991066	3.04843	5.319557	-1.92993
QG13 (MVAr)	-15	44	19.39047	19.22173	-6.96992	-1.56298	15.18239	6.184359	20.01357
QG24 (MVAr)	-15	44	1.063447	15.58164	3.148071	9.864174	9.647139	0.900453	13.81952
QG 30 (MVAr)	-15	44	3.716495	19.72763	14.36053	7.600432	9.55253	10.91323	2.573355
Objective function			2.409543	0.091077	804.9323	0.083975	788.6009	953.8583	895.224

Table A.3: Results of the MRFO algorithms for IEEE 30-bus network model considering 30% load increasing and line outages over different objective function cases.

Parameters	**Min**	**Max**	**case 1**	**case 2**	**case 3**	**case 4**	**case 5**	**case 6**	**case 7**
PG2 (MW)	20	80	78.94449	79.83669	65.58424	49.34778	64.66157	73.1973	63.48292
PG5 (MW)	15	50	49.98827	49.82762	28.24901	45.90088	33.82235	49.84066	49.87719
PG8 (MW)	10	35	34.95284	34.7913	34.94111	31.15215	34.70196	34.95787	34.98517
PG11 (MW)	10	30	29.91441	29.90981	27.59889	29.55048	26.5664	29.98705	29.87211
PG13 (MW)	10	40	39.64715	39.97612	26.61393	29.17901	23.9581	39.1412	39.62201
V1 (p.u.)	0.95	1.1	1.081956	1.046626	1.092108	1.032217	1.062568	1.083414	1.083951
V2 (p.u.)	0.95	1.1	1.065634	1.033513	1.07761	1.014742	1.047367	1.072297	1.068344
V5 (p.u.)	0.95	1.1	1.036057	0.975877	1.03372	1.015921	1.020408	1.033834	1.033085
V8 (p.u.)	0.95	1.1	1.028779	0.999667	1.028509	1.001257	1.005163	1.033002	1.030437
V11 (p.u.)	0.95	1.1	1.087029	1.025528	1.072146	1.058847	1.004218	1.099288	1.071498
V13 (p.u.)	0.95	1.1	1.074987	1.067463	1.06855	1.041078	1.031964	1.052367	1.03801
QC10 (MVAr)	0	5	2.177567	1.962423	1.950354	3.681026	2.871682	1.97668	3.38373
QC12 (MVAr)	0	5	2.481772	2.836509	1.480597	0.935936	1.233784	2.44054	3.154654
QC15 (MVAr)	0	5	3.31715	3.297904	1.615822	4.297911	4.458261	2.921722	2.236931
QC17 (MVAr)	0	5	3.419588	2.124557	4.202032	3.147542	2.587714	2.516494	4.877759
QC20 (MVAr)	0	5	1.463249	3.964579	3.48587	4.568082	4.801797	3.555862	4.260357
QC21 (MVAr)	0	5	4.442144	2.293983	4.699624	4.451532	4.797764	4.602726	4.447628
QC23 (MVAr)	0	5	2.098127	3.903728	4.077244	3.812175	4.702557	4.534655	4.044118
QC24 (MVAr)	0	5	3.978503	2.174635	3.624665	4.382269	4.877549	4.777324	4.816797
QC29 (MVAr)	0	5	2.999428	2.916789	2.686182	2.103919	1.377672	3.194547	1.678429
T11 (p.u.)	0.9	1.1	1.020357	1.037524	1.039978	1.065708	1.013077	1.032093	1.094004
T12 (p.u.)	0.9	1.1	0.948111	0.947277	0.942346	0.901865	0.903039	0.932736	0.939791
T15 (p.u.)	0.9	1.1	1.011039	0.987815	0.987828	1.010391	1.007613	0.984559	1.017915
T36 (p.u.)	0.9	1.1	0.983533	0.970228	0.97034	0.937559	0.940359	0.965428	0.96658
PG1 (MW)	50	200	145.3291	145.484	199.8753	197.7545	199.8073	151.7441	161.408
QG1 (MVAr)	-20	150	6.661507	0.288621	-3.58019	-10.343	-3.42034	-3.86065	2.050774
QG2 (MVAr)	-20	60	4.90321	27.79252	34.9193	-3.86528	24.35985	25.46731	16.21581
QG5 (MVAr)	-15	62.5	32.43408	7.452135	32.63462	57.48644	48.53358	25.35044	27.06184
QG8 (MVAr)	-15	48	22.4029	39.95048	24.79764	37.36931	42.24075	28.13959	23.54894
QG11 (MVAr)	-10	40	24.14658	16.54514	21.33558	28.86264	1.732175	28.61334	31.55477
QG13 (MVAr)	-15	44	21.06083	28.217	14.68961	19.23051	13.22439	3.776342	9.982602
Objective function			10.35625	0.287071	1072.905	0.203117	1193.317	1633.216	1249.935

Table A.4: Results of the MRFO algorithms for Modified (1) network model considering 30% load increasing and line outages over different objective function cases.

Parameters	Min	Max	case 1	case 2	case 3	case 4	case 5	case 6	case 7
PG2 (MW)	20	80	78.96897	77.98696	47.31534	48.92198	51.63177	59.07841	65.6926
PG5 (MW)	15	50	49.75286	49.78734	23.48595	39.71887	29.70946	46.63523	41.52254
PG8 (MW)	10	35	34.58978	34.97955	17.62082	27.82599	31.92295	33.85609	27.52136
PG11 (MW)	10	30	29.88365	29.93845	25.4378	22.95243	25.80333	26.38364	25.23275
PG13 (MW)	10	40	39.67939	39.83336	31.83106	23.71102	21.67895	32.93794	38.35061
PG24 (MW)	10	30	34.64945	31.31808	31.94187	22.04308	29.94312	33.81893	29.67559
PG30 (MW)	10	40	23.33483	34.99725	17.84804	17.97953	19.7405	24.47107	20.12121
V1 (p.u.)	0.95	1.1	1.063925	1.07387	1.054677	1.033922	1.030842	1.060292	1.063462
V2 (p.u.)	0.95	1.1	1.053655	1.067041	1.038821	1.022276	1.007517	1.055784	1.055167
V5 (p.u.)	0.95	1.1	1.024181	1.012364	0.988563	1.021867	0.968974	1.021903	1.009547
V8 (p.u.)	0.95	1.1	1.034577	1.021702	1.003073	0.993468	0.996842	1.008956	1.029904
V11 (p.u.)	0.95	1.1	1.043691	1.030491	1.041562	1.045414	1.070071	1.026937	1.057706
V13 (p.u.)	0.95	1.1	1.077659	1.035777	1.054522	0.997822	1.017527	1.021037	0.991366
V24 (p.u.)	0.95	1.1	1.033488	1.022621	1.017592	1.030418	1.030332	1.017659	1.018034
V30 (p.u.)	0.95	1.1	1.038833	1.08252	0.994157	0.994472	0.994693	1.034226	1.006218
QC10 (MVAr)	0	5	2.278882	3.132612	2.890755	2.501674	2.754704	0.461179	2.615473
QC12 (MVAr)	0	5	0.164793	3.402865	1.885262	4.178705	3.042388	2.514137	3.18184
QC15 (MVAr)	0	5	2.151162	3.413179	3.718069	4.228252	4.548734	3.441233	4.032904
QC17 (MVAr)	0	5	3.869799	0.4709	3.96408	2.79627	2.395369	1.743567	3.710018
QC20 (MVAr)	0	5	1.466611	3.409901	1.571531	4.73299	2.140893	4.490369	3.462153
QC21 (MVAr)	0	5	2.443377	2.454726	2.780677	3.811369	3.762391	2.048941	1.977807
QC23 (MVAr)	0	5	1.096695	3.068933	1.543831	0.19635	0.873228	1.838742	1.577679
QC24 (MVAr)	0	5	2.106778	3.063475	2.111643	2.26522	2.396395	0.581908	1.560782
QC29 (MVAr)	0	5	3.347535	4.742404	2.322185	3.25545	3.559147	2.761782	3.082734
T11 (p.u.)	0.9	1.1	0.986026	0.972644	1.00365	1.058723	1.008261	0.951534	1.004849
T12 (p.u.)	0.9	1.1	0.978386	0.951062	1.034732	0.954365	1.032838	1.051182	0.981354
T15 (p.u.)	0.9	1.1	1.035464	1.035861	1.036447	0.964705	0.986375	0.975444	1.05668
T36 (p.u.)	0.9	1.1	1.017255	1.093388	0.956061	1.014009	0.978366	1.005584	1.015467
PG1 (MW)	50	200	82.9277	75.77557	185.0096	176.9115	169.1525	118.2156	128.1961
QG1 (MVAr)	-20	150	0.405601	3.19481	-7.44534	-14.2802	7.484293	-9.77482	-11.5805
QG2 (MVAr)	-20	60	2.500786	32.12949	29.64943	11.29931	1.511998	39.32977	27.98602
QG5 (MVAr)	-15	62.5	25.32738	10.97833	22.30958	62.13944	22.48241	35.20044	16.30698
QG8 (MVAr)	-15	48	26.91915	11.99124	24.70083	12.56644	31.74416	20.24748	35.9639
QG11 (MVAr)	-10	40	3.809973	-0.1999	15.79635	23.50413	28.2527	1.530513	16.65041
QG13 (MVAr)	-15	44	30.02298	12.62193	28.29841	-7.94096	5.761604	2.035944	0.653175
QG24 (MVAr)	-15	44	8.680901	9.336052	13.45444	30.27236	24.18245	12.91652	17.56532
QG 30 (MVAr)	-15	44	0.416866	11.97251	-6.58519	-2.47701	-6.08521	1.754381	-2.46631
Objective function			5.366639	0.106125	1097.801	0.086139	1077.842	1360.785	1267.739

Table A.5: Results of the MRFO algorithms for Modified (2) network model considering 30% load increasing and line outages over different objective function cases.

Parameters	Min	Max	case 1	case 2	case 3	case 4	case 5	case 6	case 7
PG2 (MW)	20	80	79.00149	74.8635	46.6811	58.22198	50.83562	67.40784	51.17015
PG5 (MW)	15	50	49.47831	49.16434	28.34376	45.4369	31.02998	45.63023	44.54412
PG8 (MW)	10	35	34.6971	34.3292	17.23866	15.10945	29.61125	34.43795	32.73215
PG11 (MW)	10	30	29.16752	29.64316	20.01942	28.19089	18.53591	22.8976	22.97138
PG13 (MW)	10	40	39.50936	39.80338	25.01644	25.12719	34.84481	37.63715	31.42468
PG24 (MW)	10	30	34.07383	34.96276	25.61198	24.15306	28.82371	27.45107	28.10106
PG30 (MW)	10	40	33.05256	34.29304	23.45599	26.22933	24.28776	30.16446	28.09945
V1 (p.u.)	0.95	1.1	1.063334	1.072434	1.035254	1.025283	1.085124	1.067451	1.059591
V2 (p.u.)	0.95	1.1	1.056744	1.057138	1.0177	1.009935	1.04946	1.049982	1.035092
V5 (p.u.)	0.95	1.1	1.019907	0.984366	0.973253	1.01703	0.964841	1.005012	0.998674
V8 (p.u.)	0.95	1.1	1.038759	1.012435	0.984456	0.994805	0.997273	1.025395	1.004556
V11 (p.u.)	0.95	1.1	1.066567	1.048274	1.054442	1.034212	1.068435	1.02458	1.002695
V13 (p.u.)	0.95	1.1	1.054095	1.052389	0.994329	1.005019	1.033426	1.035493	1.011156
V24 (p.u.)	0.95	1.1	1.040507	1.00883	1.002526	1.032926	1.029804	1.011434	1.012037
V30 (p.u.)	0.95	1.1	1.054074	1.033843	1.027541	1.031024	1.0221	1.039485	1.007327
QC10 (MVAr)	0	5	2.493709	3.336323	2.141834	2.494784	3.367212	1.518972	2.56503
QC12 (MVAr)	0	5	2.796687	2.538229	1.340885	1.852237	1.916065	3.411	2.733211
QC15 (MVAr)	0	5	2.57427	2.061078	3.566731	3.349961	3.113586	2.608734	1.952866
QC17 (MVAr)	0	5	2.433391	3.447538	3.248285	1.329277	2.590277	1.904918	1.719682
QC20 (MVAr)	0	5	0.731748	1.642465	1.309861	4.75354	4.680383	2.969138	1.695451
QC21 (MVAr)	0	5	2.021231	3.851081	2.89671	4.955263	2.775167	2.802972	1.066731
QC23 (MVAr)	0	5	2.919978	1.362881	2.568006	4.745201	3.351246	1.877524	0.853848
QC24 (MVAr)	0	5	1.153299	4.537772	2.9841	3.621478	0.775302	2.2439	3.068872
QC29 (MVAr)	0	5	2.492457	2.121194	3.03757	4.016321	3.150069	2.271534	4.297433
T11 (p.u.)	0.9	1.1	1.009383	0.967195	1.034364	1.077024	1.071996	0.992497	0.962727
T12 (p.u.)	0.9	1.1	0.980484	1.050467	0.991304	0.903831	1.047344	0.979637	0.987968
T15 (p.u.)	0.9	1.1	0.989832	1.035925	0.975795	0.978819	0.98041	1.088445	0.996929
T36 (p.u.)	0.9	1.1	0.981204	1.024632	0.98662	1.003575	0.988041	0.996703	1.04716
PG1 (MW)	50	200	75.01545	77.68743	195.3619	156.526	161.404	109.8122	137.7088
QG1 (MVAr)	-20	150	-3.32565	21.30816	-2.86097	-6.40699	50.38176	11.32523	25.44928
QG2 (MVAr)	-20	60	15.75814	25.13243	28.89474	-9.85527	10.95306	4.282485	0.604725
QG5 (MVAr)	-15	62.5	18.38867	-6.36423	26.43162	61.86748	-9.53753	14.86808	27.79436
QG8 (MVAr)	-15	48	33.84586	14.1158	25.58473	22.02726	-0.82446	31.20136	31.35526
QG11 (MVAr)	-10	40	15.23982	10.76785	30.27025	21.09399	34.92945	4.249821	-3.39173
QG13 (MVAr)	-15	44	9.395583	25.68146	0.808552	-1.63449	7.283186	25.32366	5.557552
QG24 (MVAr)	-15	44	10.44966	4.363254	15.23614	23.27533	23.47096	11.66743	20.64932
QG 30 (MVAr)	-15	44	-3.8103	1.454174	1.820208	-0.90529	-2.92932	-0.81551	-0.30307
Objective function			7.303549	0.105623	1052.049	0.14091	1123.534	1382.903	1286.251

Table A.6: Results of the MRFO and the proposed metaheuristic optimization techniques for case 3 for the large scale power network model (IEEE 118-bus system).

Parameters	Range (unit)	AGPSO	MFO	IPSO	MRFO	SDO	ALO	CGSA
PG1	30-100 (MW)	30	30	30	30.96757	37.45242	32.19872	56.92175
PG4	30-100 (MW)	30	30	30	38.69991	37.38809	30.52256	54.72663
PG6	30-100 (MW)	30	30	30	31.88598	36.7689	32.31421	48.07277
PG8	30-100 (MW)	100	30	30	37.14882	47.54017	30.08409	59.10519
PG10	165-550 (MW)	165	344.4105	165	314.189	274.3131	321.2854	288.2645
PG12	55.5-185 (MW)	55.5	55.5	55.5	69.95526	67.56325	57.61395	61.73909
PG15	30-100 (MW)	100	30	30	32.03603	38.63409	30.99056	52.91447
PG18	30-100 (MW)	100	30.54771	30	30.20097	42.35575	64.14394	30.00004
PG19	30-100 (MW)	30	30	30	30.45038	36.98835	59.71248	56.3819
PG24	30-100 (MW)	30	30	30	36.48068	31.03371	30.58917	45.16931
PG25	96-320 (MW)	96	96.00857	175.0428	151.1618	147.5557	149.6173	160.4091
PG26	124.2-414 (MW)	231.1613	240.997	254.2534	212.8986	206.1774	172.494	254.7575
PG27	30-100 (MW)	30	30	30	32.73291	30.98495	43.6923	63.56414
PG31	32.1-107 (MW)	32.1	32.1	32.1	32.11366	32.10476	32.1	32.1
PG32	30-100 (MW)	100	30	30	31.01471	43.87933	30.05668	57.00572
PG34	30-100 (MW)	100	30	30	31.08278	42.2081	30.04785	59.99619
PG36	30-100 (MW)	100	30	30	31.90564	32.00456	30.64935	32.58738
PG40	30-100 (MW)	30	30	30	33.07294	41.89296	36.44252	52.61235
PG42	30-100 (MW)	30	30.00002	30	30.7529	31.87347	30.04052	61.19681
PG46	35.7-119 (MW)	35.7	35.7	35.7	35.83198	36.0983	35.7	35.7
PG49	91.2-304 (MW)	91.2	175.5565	182.7174	162.0221	146.8441	114.7176	135.8814
PG54	44.4-148 (MW)	44.4	47.67372	44.4	47.18772	47.30178	45.91587	75.87834
PG55	30-100 (MW)	30	30	30	30.92842	35.85357	30.3001	40.38338
PG56	30-100 (MW)	100	30	30	34.79591	31.59644	36.30038	47.58111
PG59	76.5-255 (MW)	76.5	135.6115	76.5	120.5515	119.4002	100.0258	147.2969
PG61	78-260 (MW)	78	130.3805	140.5072	127.8258	112.2114	134.6712	131.2491
PG62	30-100 (MW)	30	30.00001	30	32.36409	33.47516	30.12824	50.602
PG65	147.3-491 (MW)	147.3	314.8029	147.3	274.2813	281.634	275.3696	264.8385
PG66	147.6-492 (MW)	147.6	147.6	330.1276	281.2701	240.7729	250.6336	277.9269
PG70	30-100 (MW)	30	30	30	30.84779	35.72794	37.26744	62.47118
PG72	30-100 (MW)	100	30.0005	100	30.86611	30.40672	30.10324	30.00293
PG73	30-100 (MW)	30	30	100	31.55323	34.93577	49.6996	62.59458
PG74	30-100 (MW)	30	30	30	31.1112	35.79324	30.02872	30.00054
PG76	30-100 (MW)	100	30.00127	30	30.56639	31.33634	35.21138	54.29059
PG77	30-100 (MW)	100	30	30	30.49904	41.72377	33.30175	59.64992
PG80	173.1-577 (MW)	173.1	355.6666	395.6407	331.2483	338.6717	318.4095	280.2968

Table A.6 Cont.

Parameters	Range (unit)	AGPSO	MFO	IPSO	MRFO	SDO	ALO	CGSA
PG85	30-100 (MW)	100	30	100	31.89674	33.34715	30.68743	30.04266
PG87	31.2-104 (MW)	31.2	31.2	31.2	31.21273	31.20615	31.2	31.2
PG89	212.1-707 (MW)	212.1	376.3453	212.1	373.7225	362.243	403.1462	365.5596
PG90	30-100 (MW)	30	100	30	31.26029	31.6276	30.00069	42.73916
PG91	30-100 (MW)	30	30	30	30.63928	40.86916	30.37009	30
PG92	30-100 (MW)	30	30	100	30.25403	37.7424	30.00787	46.64855
PG99	30-100 (MW)	30	30.02172	30	30.6721	33.00981	30.07874	30
PG100	105.6-352 (MW)	105.6	181.8163	201.5991	174.0365	136.3298	165.5598	167.2408
PG103	42-140 (MW)	42	42	42	42.65984	45.82262	42.21775	47.45191
PG104	30-100 (MW)	100	30	30	31.02069	34.54116	31.49788	45.99121
PG105	30-100 (MW)	30	30	30	30.56365	51.10086	30.1704	30.00011
PG107	30-100 (MW)	100	30	30	30.74997	30.86223	30.38378	46.66208
PG110	30-100 (MW)	30	30	30	31.04967	30.4354	30.168	33.01099
PG111	40.8-136 (MW)	40.8	40.8067	40.8	41.16207	42.51737	41.04555	40.83572
PG112	30-100 (MW)	100	30.00136	30	30.38368	30.21976	30.66641	53.14452
PG113	30-100 (MW)	30	30	30	31.79081	33.64665	30.32401	30.00368
PG116	30-100 (MW)	100	30	30	31.33014	30.24324	30.47595	61.00436
VG1	(p.u)	1.1	1.09999	1.1	0.998229	0.982739	1.029343	0.985709
VG4	(p.u)	1.1	1.099805	1.1	1.013872	0.995006	1.07073	0.995771
VG6	(p.u)	1.1	1.1	1.1	1.003335	0.991238	1.059188	1.021008
VG8	(p.u)	1.1	1.1	1.1	1.021154	0.973657	1.035121	1.021501
VG10	(p.u)	1.1	1.1	1.1	1.043335	1.014003	1.058952	1.069293
VG12	(p.u)	1.1	1.1	1.1	1.007116	0.990264	1.053148	1.024564
VG15	(p.u)	1.1	1.1	1.1	0.99871	0.976985	1.05415	1.032899
VG18	(p.u)	0.95	1.099803	1.1	1.000742	0.984192	1.063527	1.034675
VG19	(p.u)	1.1	1.1	1.1	0.991393	0.970413	1.052833	1.049455
VG24	(p.u)	1.1	1.1	1.1	1.006627	0.991053	1.033501	1.024659
VG25	(p.u)	1.1	1.1	1.1	1.003077	0.995181	1.050835	1.028193
VG26	(p.u)	1.1	1.1	1.1	1.039963	0.989802	1.056238	0.998241
VG27	(p.u)	1.1	1.099999	1.1	1.004515	0.966514	1.055823	0.969271
VG31	(p.u)	1.1	1.096255	1.1	0.997407	0.983931	1.04982	1.022014
VG32	(p.u)	1.1	1.1	1.1	1.00424	0.979768	1.042494	0.992235
VG34	(p.u)	1.1	1.1	1.1	1.004577	0.987231	1.057136	1.029457
VG36	(p.u)	1.1	1.1	1.1	1.00375	0.980783	1.054074	1.011428
VG40	(p.u)	1.1	1.082856	1.1	0.992705	0.970891	1.044673	1.030762
VG42	(p.u)	1.1	1.077736	1.1	0.984555	0.969592	1.056026	1.040734

Table A.6 Cont.

Parameters	Range (unit)	AGPSO	MFO	IPSO	MRFO	SDO	ALO	CGSA
VG46	(p.u)	1.1	1.1	1.1	0.97959	0.984637	1.055091	1.025712
VG49	(p.u)	1.1	1.097394	1.1	0.982181	0.987269	1.069266	1.020808
VG54	(p.u)	1.1	1.052031	1.1	0.965236	0.961004	1.05932	0.991423
VG55	(p.u)	1.1	1.04899	1.1	0.962025	0.955332	1.060495	1.022598
VG56	(p.u)	1.1	1.04833	1.1	0.964113	0.959133	1.059448	0.985944
VG59	(p.u)	1.1	1.064989	1.1	0.984881	0.969187	1.066789	1.013321
VG61	(p.u)	1.1	1.084577	1.1	0.984874	0.982994	1.061875	1.035536
VG62	(p.u)	1.1	1.085795	1.1	0.979581	0.980883	1.057629	1.031393
VG65	(p.u)	1.1	0.95	1.1	0.989528	0.966526	1.068715	1.022879
VG66	(p.u)	1.1	1.099602	1.1	0.986523	0.979194	1.081559	1.045484
VG70	(p.u)	1.1	1.1	1.1	1.007477	1.001306	1.058688	1.002377
VG72	(p.u)	1.1	1.1	1.1	0.997136	0.986891	1.048889	1.054746
VG73	(p.u)	1.1	1.09922	1.1	0.990812	0.978309	1.047086	1.016771
VG74	(p.u)	1.1	1.098527	1.1	1.013918	0.977304	1.054302	1.043769
VG76	(p.u)	1.1	1.1	1.1	0.976014	0.971128	1.041931	1.021779
VG77	(p.u)	1.1	1.071125	1.1	0.970109	0.971193	1.031252	1.016732
VG80	(p.u)	1.1	1.075183	1.1	0.981236	0.995623	1.041891	1.020222
VG85	(p.u)	1.1	1.078921	1.1	0.988678	1.007653	1.051081	1.031347
VG87	(p.u)	1.1	1.1	1.1	1.005024	1.000543	1.037322	1.059626
VG89	(p.u)	1.1	1.1	1.1	0.996996	0.968108	1.049529	1.056419
VG90	(p.u)	1.1	1.1	1.1	1.01321	1.007167	1.065019	1.009426
VG91	(p.u)	1.1	1.1	1.1	0.997392	0.990586	1.05495	1.034428
VG92	(p.u)	1.1	1.1	1.1	0.99747	0.986943	1.05824	1.040041
VG99	(p.u)	1.1	1.094449	1.1	1.006164	0.997758	1.064785	1.01001
VG100	(p.u)	1.1	1.1	1.1	0.972062	0.992236	1.055319	1.048106
VG103	(p.u)	1.1	1.070245	1.1	0.992506	1.001478	1.063885	1.033873
VG104	(p.u)	1.1	1.055268	1.1	0.997462	1.00344	1.065813	1.024946
VG105	(p.u)	1.1	1.025686	1.1	1.004403	1.011794	1.052274	1.004192
VG107	(p.u)	1.1	1.01719	1.1	1.009979	1.005123	1.049861	1.014309
VG110	(p.u)	1.1	0.95	1.1	1.003936	1.003016	1.046556	0.957684
VG111	(p.u)	1.1	1.06465	1.1	1.008132	1.003809	1.057257	1.027574
VG112	(p.u)	1.1	1.1	1.1	1.011296	1.006388	1.062672	1.052127
VG113	(p.u)	1.1	1.066452	1.1	1.000952	0.99998	1.052244	1.012115
VG116	(p.u)	1.1	1.099998	1.1	1.019567	1.003468	1.066107	1.021668
QC5	(MVAr)	1.1	0.95	1.1	0.992519	0.990879	1.054895	1.01871
QC34	(MVAr)	25	24.60774	25	14.23945	6.987025	5.61805	11.8448

Table A.6 Cont.

Parameters	Range (unit)	AGPSO	MFO	IPSO	MRFO	SDO	ALO	CGSA
QC37	(MVAr)	25	0	25	7.777117	7.027916	0.803327	16.59707
QC44	(MVAr)	0	25	0	8.355769	6.652553	21.9136	10.09537
QC45	(MVAr)	14.32451	9.478307	3.091401	3.698047	7.43489	8.555815	13.56792
QC46	(MVAr)	0	25	16.12487	11.76134	9.67422	0	11.54436
QC48	(MVAr)	25	3.856716	25	11.35375	8.481854	0	10.79601
QC74	(MVAr)	0	0.001562	6.161427	17.27489	4.436313	11.221	9.715015
QC79	(MVAr)	25	3.673715	25	19.69564	6.578532	0	7.03489
QC82	(MVAr)	0	25	0	12.69201	16.89946	2.863306	13.68539
QC83	(MVAr)	25	0	25	10.37409	8.390118	0.057374	10.9378
QC105	(MVAr)	25	24.72202	8.559449	12.17088	5.511948	15.28833	9.784053
QC107	(MVAr)	13.7981	25	25	12.19842	8.335438	14.89733	14.15661
QC110	(MVAr)	25	25	0.097001	6.715803	7.125564	3.207183	10.56264
TS8	(p.u)	1.1	1.1	1.1	0.981506	0.978347	0.969248	0.949922
TS32	(p.u)	1.1	0.9	1.1	0.97291	0.933048	0.971081	1.021558
TS36	(p.u)	1.1	0.957863	1.1	0.971023	0.954292	0.987372	1.018254
TS51	(p.u)	0.9	0.924651	1.1	0.942711	0.970844	0.994566	0.982483
TS93	(p.u)	0.966503	0.9	1.1	0.93619	1.007349	0.979119	1.001944
TS95	(p.u)	1.1	0.900001	1.1	1.013301	0.949085	1.01507	1.044051
TS102	(p.u)	1.1	0.9	1.1	1.002486	1.035996	1.015126	1.099689
TS107	(p.u)	1.1	0.900581	1.1	0.98146	1.00364	1.004581	0.996547
TS127	(p.u)	1.1	0.90317	1.1	0.991761	1.008993	0.990989	0.981716
PG69	MW	413.2441	402.9867	417.4569	369.2255	376.5373	421.7667	-132.246
Objective function		146423.6	136484.9	139380.6	135606.5	136708.1	136122.5	144811.7